FLEXURAL BEHAVIOUR OF REINFORCED CONCRETE BEAMS WITH A LAYER OF SHCC IN THE TENSION ZONE – Numerical Study by ATENA Model

Final Report

MSc ADDITIONAL THESIS

N. JAYANANDA

4619617

SEPTEMBER 2017

Faculty of Civil Engineering and Geosciences (CEG). Delft University of Technology

Acknowledgements.

It is during the toughest times that you are truly aware of your true strength and resolve.
The past one year in Delft University of Technology has been a challenging yet one amazing year. It has taught me lessons that I will carry with me not only in the next year of my Masters Programme but for the rest of my life. So thank you TU Delft for this unforgettable experience.

My first thank you goes to the Civil Engineering Department especially the Concrete Structures faculty for allowing me to pursue the MSc. Additional thesis course which has been a short yet a very insightful journey.

I am grateful to **Prof.dr.ir** D.A. Hordijk and **Prof.dr.ir** H.E.J.G. Schlangen for being my supervisors for this Additional thesis. I thank Dr. Mladena Luković whole heartedly for her amazing support and insights throughout this thesis. She has been really an amazing supervisor to work with. You have truly inspired and motivated me with your knowledge on Concrete Structures. Thank you so much Mladena and I hope we can continue our association with my Master Graduation thesis as well.

I also want to thank Mr. Zhekang Huang for letting me be a part of his testing and for being so kind to share his results with me. Thank you for this Zhekang and Good luck with your Master Thesis Defense. I am forever grateful to my friends and classmates for sharing with me this incredible year at Delft. I am grateful to Mr. Dobromil and Mrs. Tereza for their guidance and help with the use of ATENA. They are always ready to answer my questions and clear my doubts.

I thank my parents for their trust and continued support. My final thanks goes to my girlfriend Chandana Jois for her endless support and motivation in my toughest times. She has loved me and cared for me through all these times, making me forever grateful to her.

Contents

List of figures.

List of Tables.

List of Abbreviations.

DIC	Digital Imaging Correlation.
ECC	Engineered Cementitious Composite.
HPFRCC	High Performance Fibre Reinforced Cementitious Composite.
LVDT	Linear Variable Displacement Transformer.
NSC	Normal Strength Concrete**.**
OPC	Ordinary Portland Cement.
SHCC	Strain Hardening Cementitious Composite.
SLS	Serviceability Limit State.
RB	Reinforced Concrete Beam.
ULS	Ultimate Limit State.

List of Symbols.

Roman Lower Case Letters

$f_{cm,\ cube}$	Mean Cube Compressive Strength.
f_{cm}	Mean Cylindrical Compressive Strength.
f_{t1}	Mean Tensile Strength.
f_{t2}	Ultimate Tensile Strength.
f_t	Interface Tensile Strength.

Roman Capital Letters

C	Interface Cohesion.
E	Young's Modulus of Elasticity.
K_{nn}	Normal Stiffness of Interface.
K_{tt}	Shear Stiffness of Interface.

Greek Letters

ε_1	Elastic Strain Capacity
ε_2	Ultimate Strain Capacity.
γ	Specific Density.
Ø	Diameter of Reinforcement Bar

1 General Introduction

1.1 Material SHCC.

Strain Hardening Cementitious Composite (SHCC) is a new generation of cement based building material characterized by increased ductility and improved cracking behavior in comparison to the traditional concrete. This is attributed to the special material composition (no coarse aggregates are used) and crack bridging ability of the fibers which are added in the composite and act as reinforcement. Under uniaxial tension, the SHCC exhibits pseudo-strain hardening behavior with multiple cracking formation and with crack widths smaller than 100 micron [1] [2]. The high ductility and strain capacity of SHCC are exceptional for cement based materials (Figure 1.1 & Figure 1.2). They give this material a marked potential for use in applications in which high deformability is needed [3].

In conventional Reinforced concrete beam (RB), the concrete in the tension zone resists tensile forces until cracking (Crack Formation stage). Successively, at the location of cracking, the concrete cannot resist tensile forces anymore and the steel reinforcement takes up the tensile forces. Depending on the design (amount of reinforcement and its distribution), under flexural loading, the beam usually fails either by yielding of reinforcement or crushing of concrete. When SHCC is used on the tension side, due to its strain hardening behavior (even after cracking and up to a strain of approximately 5%, depending on the mixture), the entire cross-section including the SHCC layer resists the tensile forces. This means that SHCC can transfer tensile forces even after stain in the reinforcement reaches its yielding limit of around 2%. As a result, under the same bending moment, the tensile stress in the reinforcement is lower compared to that in comparative RB (with the same cross section and the amount of reinforcement). Therefore, the flexural capacity of the beam with the SHCC layer can be potentially higher than the capacity of comparative RB beam. Due to its micro cracking behavior and small crack widths, using SHCC in the tension zone, can be also possibly beneficial for durability reasons.

Under the same bending moment, the neutral axis of a cross-section having SHCC on the tension side shifts towards the tension side relative to normal reinforced concrete, increasing the depth of compression zone in concrete. In other words, having SHCC on the tension zone has the same effect as having an increased cross-sectional area of tensile reinforcement [4].

Figure 1.1 High Ductile behavior of SHCC [5].

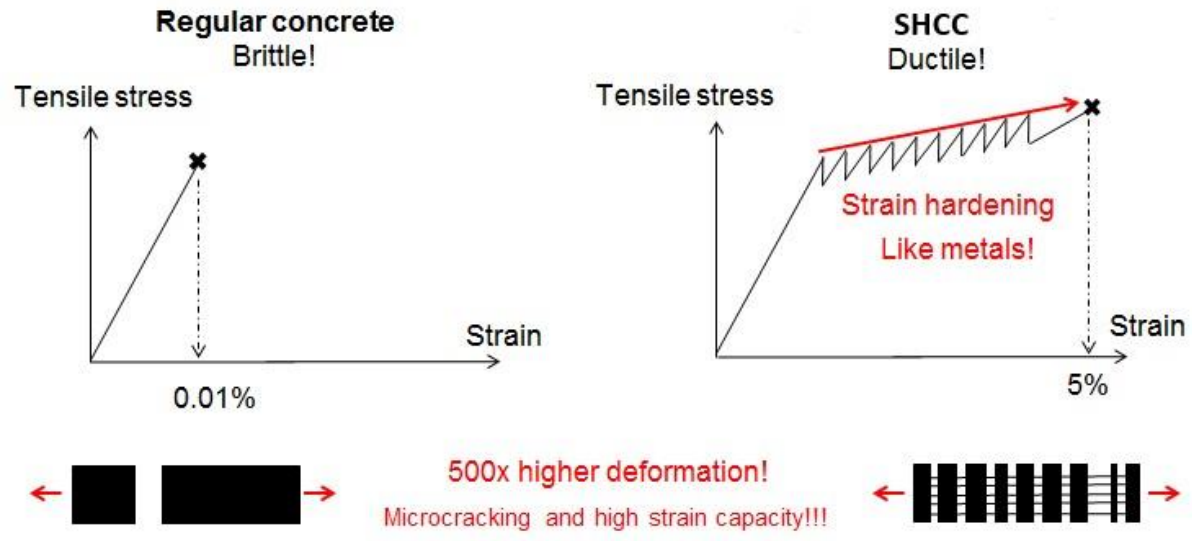

Figure 1.2 Strain Capacity of Regular Concrete and SHCC.

In the literature different names are used for more or less the same kind of material: ECC (Engineered Cementitious Composite), SHCC (Strain Hardening Cementitious Composite), HPFRCC (High Performance Fiber Reinforced Cementitious Composites), Bendable concrete etc. The basic idea for all these materials is the same and consists of designing a material with multiple cracking behavior and ductility higher than 0.5% [5]. In this thesis the name SHCC is used.
There is a great variety in types of SHCC (Table 1-1), with tensile strength capacity ranging from 3-12 MPa and ultimate strain capacity ranging from 0.5% to 8%.

Table 1-1 The range of properties for different types of SHCC [6].

Compressive Strength (MPa)	**First Crack Strength (MPa)**	**Ultimate Tensile Strength (MPa)**	**Ultimate Tensile Strain (%)**	**Young's Modulus (GPa)**	**Flexural Strength (MPa)**	**Density (Kg/m^3)**
20 - 95	3 – 7	3 - 12	0.5 – 8	18 - 24	10 - 30	950 – 2300

In this research, SHCC with an Ultimate tensile strength of 3.5 MPa and strain capacity of 3% is used [7]. The Young's Modulus (E) of the mixture is 18 GPa and Density is 2100 Kg/m^3. .

1.2 Composition.

SHCC is a mix of water, cement, fine sand, fibers and chemical additives (for example superplasticizer). It is a cementitious material and does not contain coarse aggregates, the maximum size of aggregates is about 200 μm [8]. The cement composition contains mostly Ordinary Portland cement (OPC) with additives like Fly Ash, Blast Furnace Slag and Silica Fume. The basis of using OPC is because SHCC is mostly made in the USA and Japan where OPC is most common to use. In The Netherlands mostly CEMIII/B cement (contains around 60 – 80% of slag) is used, just like the SHCC mixtures of the Delft University of Technology. The high strain capacity and crack width control are obtained by the use of PVA fibers and this special composition of the mix. The fibers are mostly made of polyvinyl alcohol (PVA), polyethylene (PE) and polypropylene (PP). In general a volume fraction of 2% of fibers is used [9].

1.3 Material Properties.

The material properties of SHCC used in research are compared with the properties of Normal strength concrete (NSC) that has a similar mean compressive strength. In the comparison a NSC of class C20/25 is used.
Table shows the comparison between NSC and SHCC used in the research (Table 1-2).

Table 1-2 Comparison of material properties of SHCC and NSC.

PROPERTY	SHCC	NSC	UNIT
Concrete Class	-	C 20/25	N/mm^2
Mean Compressive Strength, f_{cm}	32	35	N/mm^2
Young's Modulus E	18000	30000	N/mm^2
Mean Tensile Strength, f_{t1}	3.0	2.2	MPa
Ultimate Tensile Strength, f_{t2}	3.5	-	MPa
Elastic Strain Capacity, ε_1	0.1	0.1	%
Ultimate Strain Capacity, ε_2	3	0.2	%
Specific Density, γ	2100	2400	Kg/m3

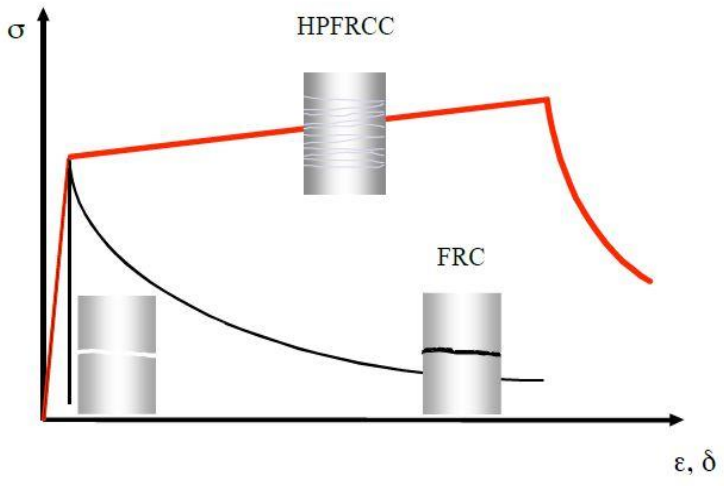

Figure 1.3 Uniaxial tensile stress-deformation relation of Normal concrete, fibre reinforced concrete (FRC) and High Performance Fiber Reinforced Cementitious Composites (HPFRCC) [6].

2 Project Framework

2.1 Project Motivation and Background.

Traditionally, reinforced concrete beams are provided with steel reinforcement in the tension zone to increase the tensile capacity of the beam since concrete is weak in tension. The reinforcement not only needs to satisfy Ultimate Limit State (ULS) conditions (i.e., is the capacity) but also the Serviceability Limit State (SLS) criteria which is mainly to limit the crack widths. Large cracks are detrimental to the functionality of the beam and can lead to durability problems.

In order to control the crack width, besides the reinforcement needed to satisfy ULS criteria, usually additional reinforcement is required in order to keep cracks small and satisfy SLS criteria. There is a possibility to avoid this by using SHCC in the tensile zone which can help reduce the crack width by smearing large cracks into many fine cracks. In this way, SHCC is used only at locations where needed: in the tension zone, around reinforcement in order to keep crack widths small. This is also economically viable because SHCC costs more than four times as much as normal concrete and therefore it is justifiable to use it only where it's more beneficial and highly effective. Using the above approach the need to use additional reinforcement for crack width control might be possibly eliminated which would result in a better optimized design.

In this thesis, benefits of using SHCC in the tension zone are investigated numerically. A comparison is made between beams made of reinforced, normal strength concrete and the beams where the reinforcement in the tension zone is embedded in a layer of SHCC. The cover thickness of the normal concrete and SHCC is varied. Numerical results are compared with experimental results with respect to the load capacity and cracking behavior (crack development, crack widths and crack spacing).

2.2 Research Layout

The research is aimed to investigate the possible benefits of ductile behavior of SHCC as compared to conventional concrete in the tension zone. Furthermore, with varying SHCC cover thickness it can be determined if the crack width can be controlled with increasing the thickness of the SHCC layer. Research Layout.

4 beams were modelled in the research and they were exposed to 4 point bending test (Figure 2.1 & Figure 2.2). 2 beams were modelled as conventional reinforced concrete beams (with the concrete cover of 11mm and 31 mm, Figure 2.3) and 2 beams with SHCC in the tension zone (with the SHCC cover of 11 mm and 31 mm, Figure 2.4).

The length of beams are 1.5m. Steel plates are used for loading and support. A schematic representation of the beam is shown in the Figure 2.1.

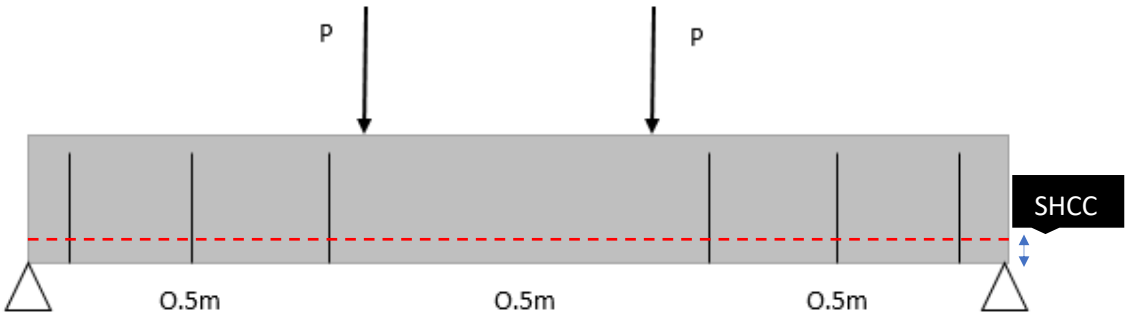

Figure 2.1 Schematic representation of the beam subjected to 4 Point Bending test with the location of the stirrups as the shear reinforcement.

Figure 2.2 Experimental Setup of the Four Point Bending Test Performed by Mr. Zhekang Huang.

2.2.1 Setup Specifications:

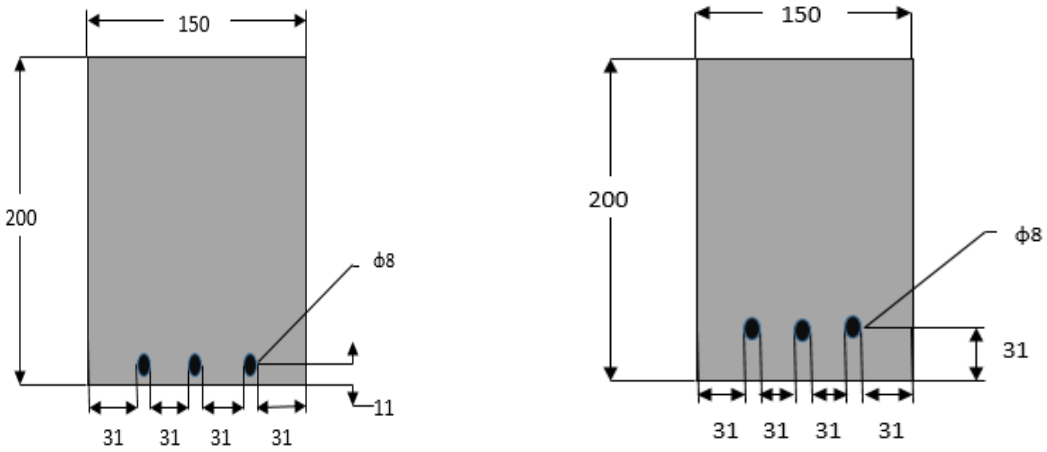

Figure 2.3 Normal RB with 11mm cover (left) and Normal RB with 31mm cover (right).

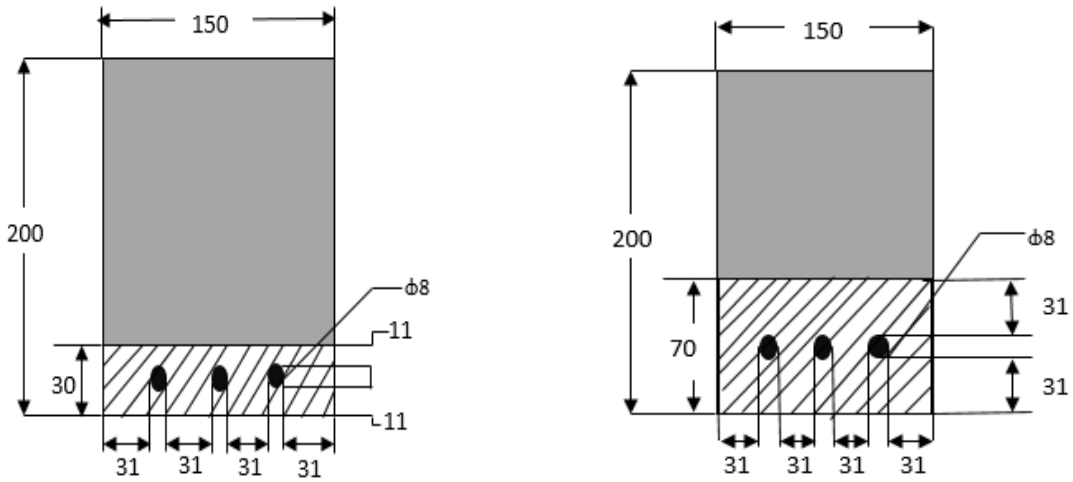

Figure 2.4 Reinforced Beam with 31mm SHCC (left) and 70mm SHCC cover (right).

2.2.2 Shear reinforcement for Beams.

If made without shear reinforcement, the beams are expected to fail in shear near the supports. Therefore, the shear reinforcement is provided in the form of stirrups. The specifications are shown in Figure 2.5 & Figure 2.6.

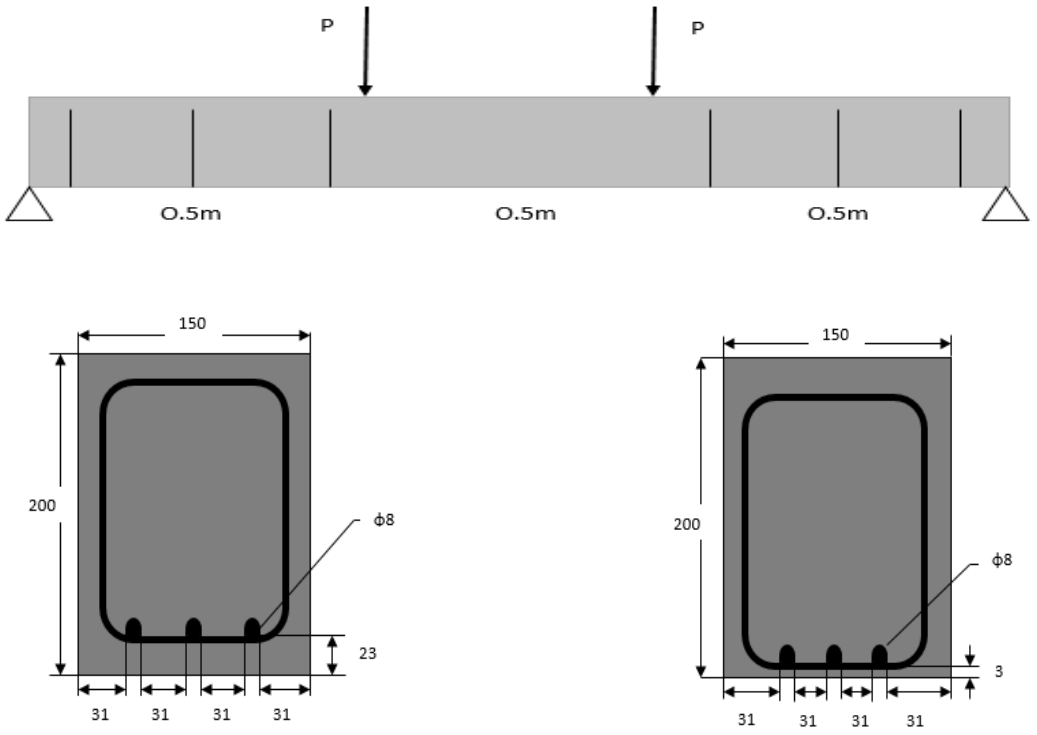

Figure 2.5 Shear Reinforcement for RB with 11mm cover (left) and 30mm cover (right).

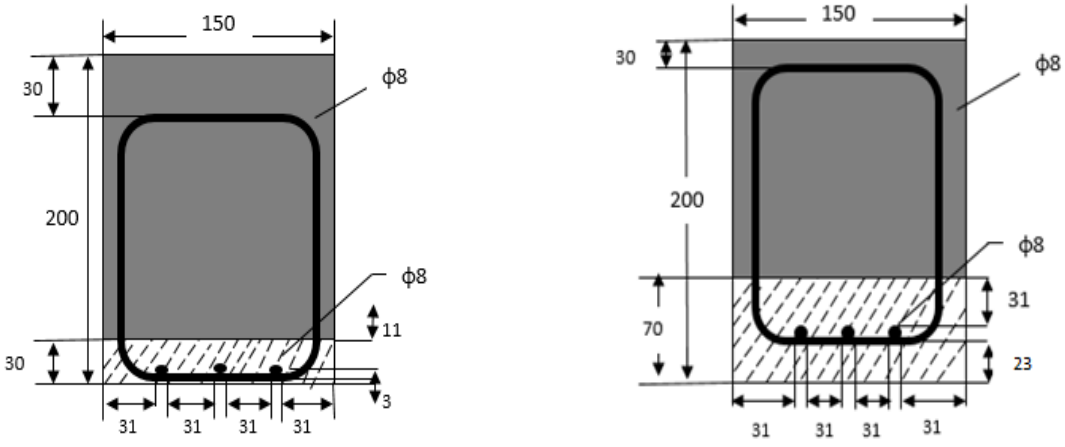

Figure 2.6 Shear Reinforcement for RB with 31mm (left) and 70mm SHCC cover (right).

2.3 Programme Used for Simulation: ATENA

ATENA is a finite element software used in this research to numerically model reinforced concrete beams and the beams with the SHCC layer, and investigate their performance under four point bending test. ATENA is a specialized software for detailed reinforced concrete analysis. The emphasis was always on 2D/3D analysis using continuum based elements, which were enhanced by specialized 3D beam and shell elements. The programme is based on continuum approach and can perform both linear and non-linear analysis. It is constructed by Cervanka Consulting, Czech Republic. For more information see www.cervanka.cz.

Since the loading and the beam setup are symmetric, and in order to reduce the computational time, only half of the beam is modelled.

The input parameters for ATENA are the material properties of the concrete beam, the loading/supporting plates and the reinforcement.

The geometry of the model is defined first and then material properties are assigned to the appropriate elements. Three types of elements are defined:

1. Regular concrete beam or composite beam (consisting of regular concrete with a layer of SHCC).

2. Steel Plates for loading/support.

3. Reinforcement (shear and longitudinal reinforcement).

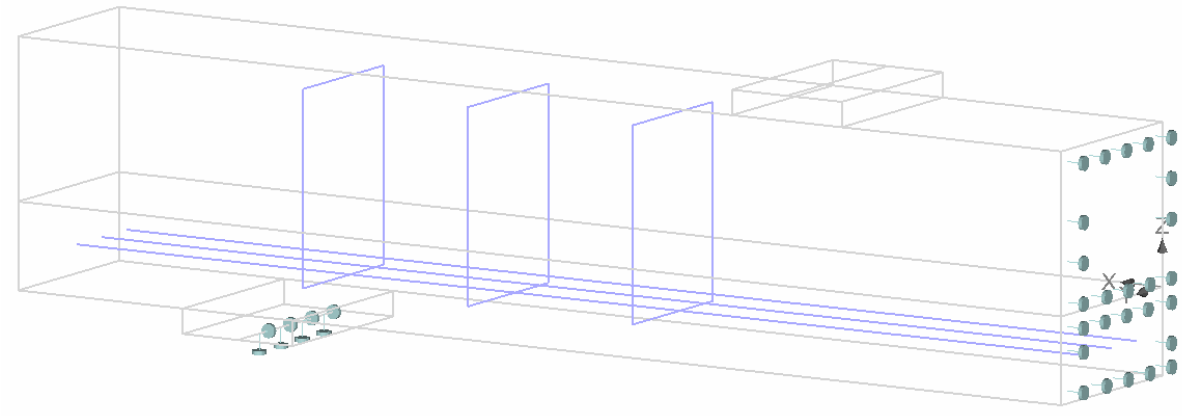

Figure 2.7 Example of ATENA model showing the half of the beam that was modelled, steel plates for loading/support (100x150x20 mm), longitudinal reinforcement (3 ø 8 mm) and shear reinforcement (3 ø 8 mm, with spacing of 150 mm). Support and conditions for symmetry.

After defining the geometry of the elements, the elements are assigned their material properties using the definition of material selection.

Definition of Concrete Properties in ATENA.

The compressive properties of concrete are based on the compressive tests performed by Mr. Zhekang Huang. The tests result are shown in Table 2-1. The mean cylinder concrete compressive strength was used as input in simulations.

Table 2-1 Results of Cube Compression Test.

Mean Cube Compressive Strength measured $f_{cm,\ cube}$ in MPa	Mean Cylindrical Compressive Strength f_{cm} in MPa (0.8 x $f_{cm,\ cube}$)
44	35

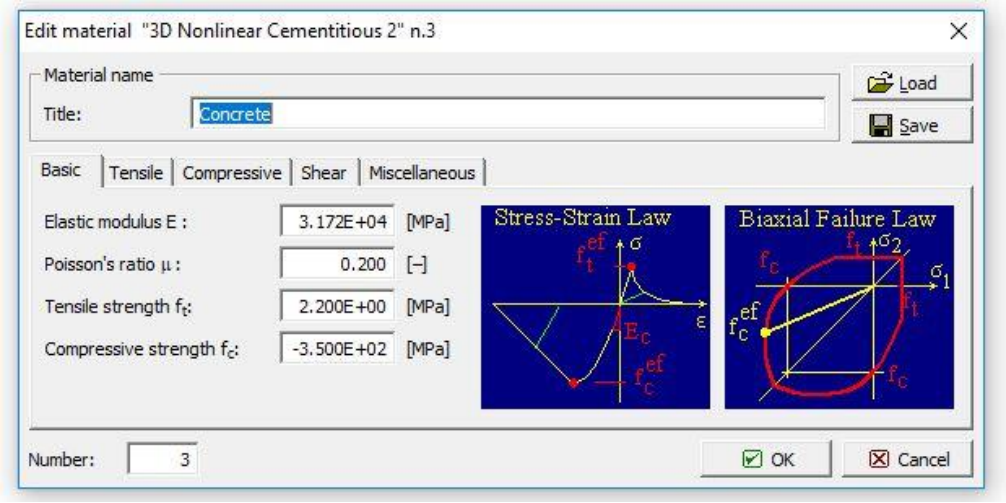

Figure 2.8 Basic Properties of Concrete.

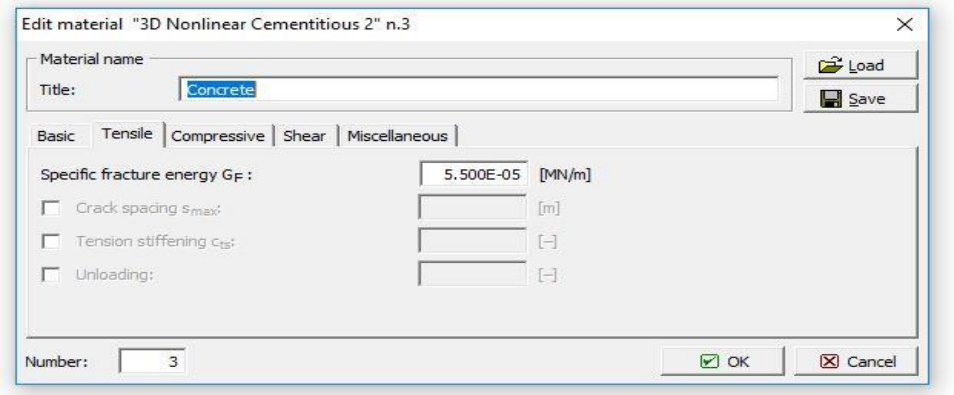

Figure 2.9 Tensile Properties of Concrete.

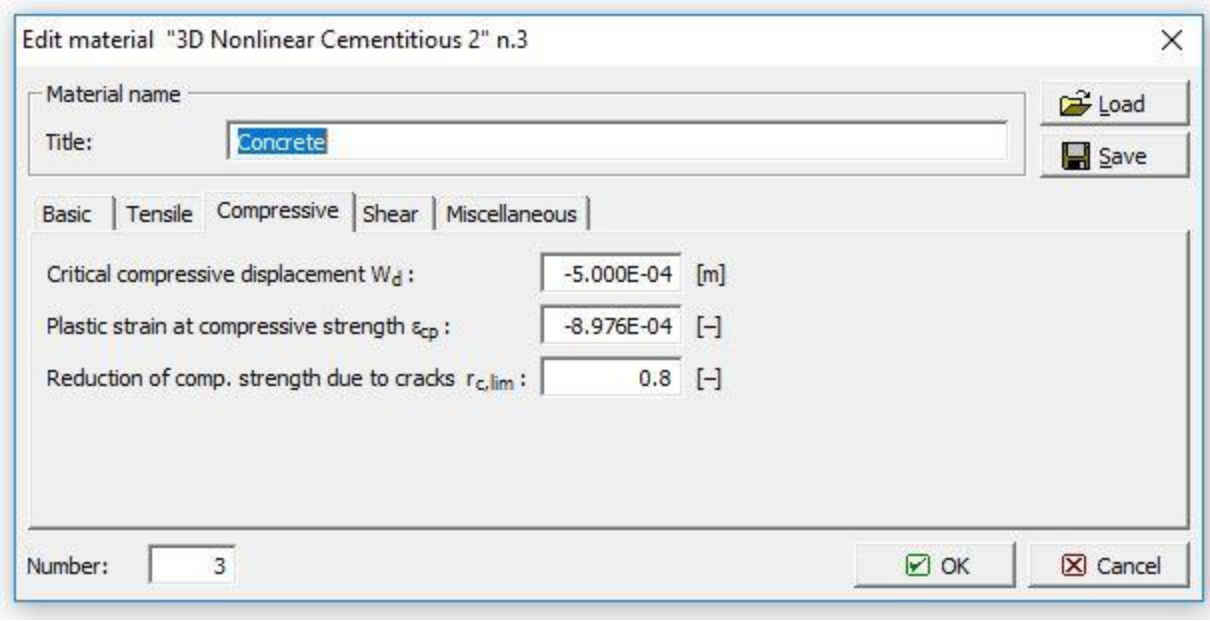

Figure 2.10 Compressive Properties of Concrete.

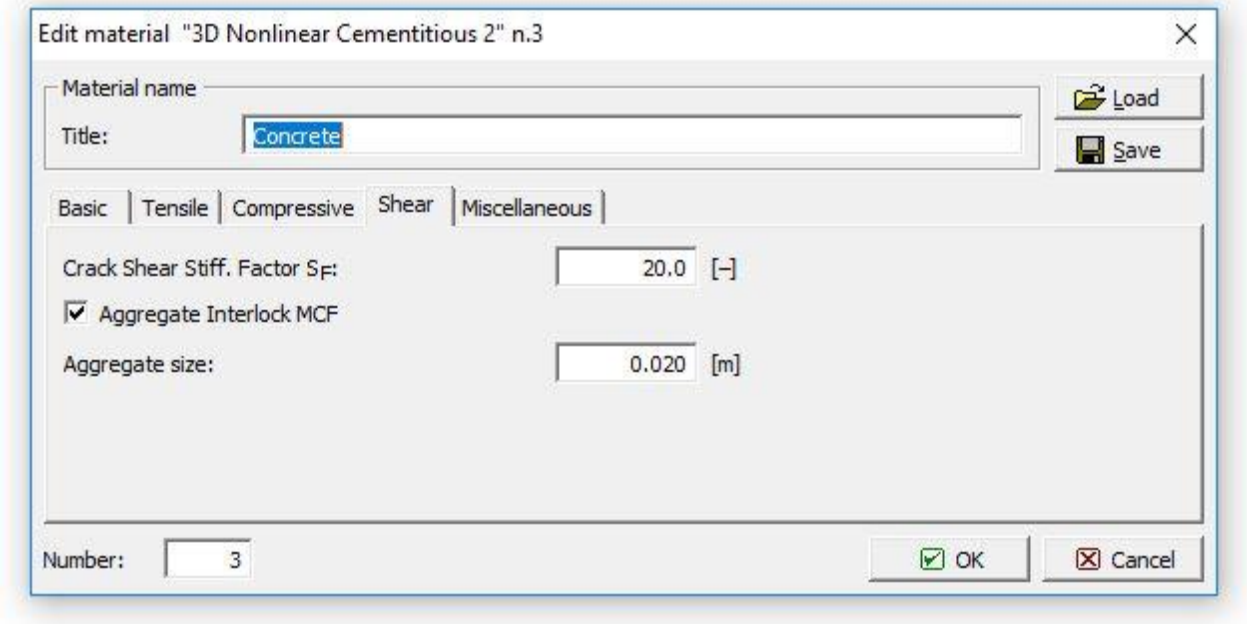

Figure 2.11 Shear Properties of Concrete.

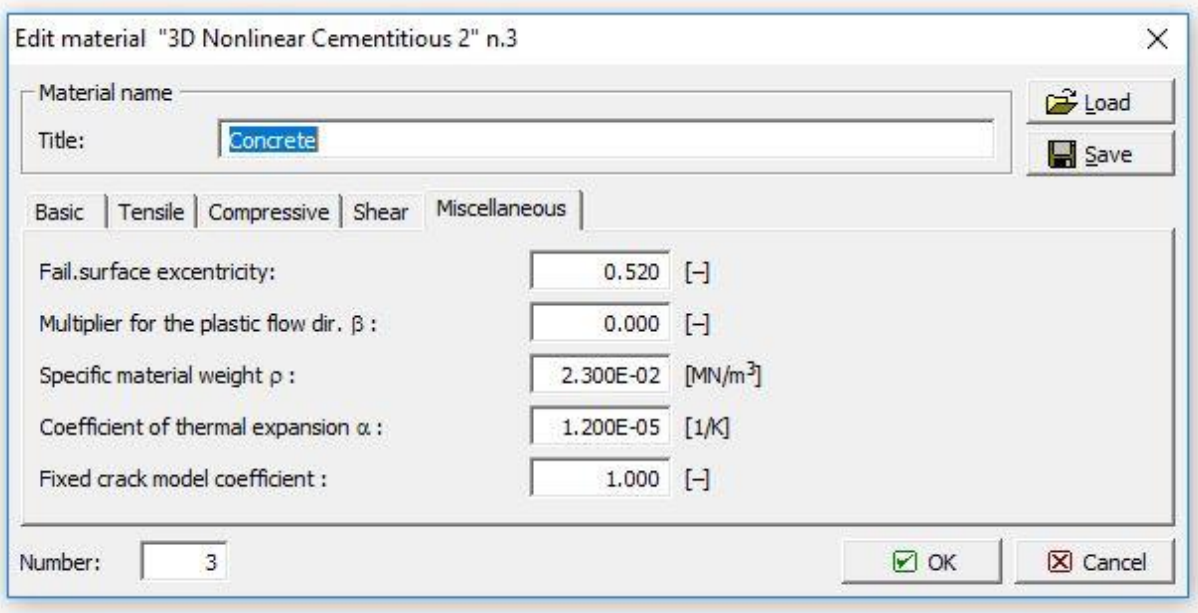

Figure 2.12 Miscellaneous Properties of Concrete.

Steel plates are used for both loading and support. The material definition of these plates is shown below.

Definition of Material Properties for Steel plates

Properties for the steel plates are assumed based on the known properties of steel.

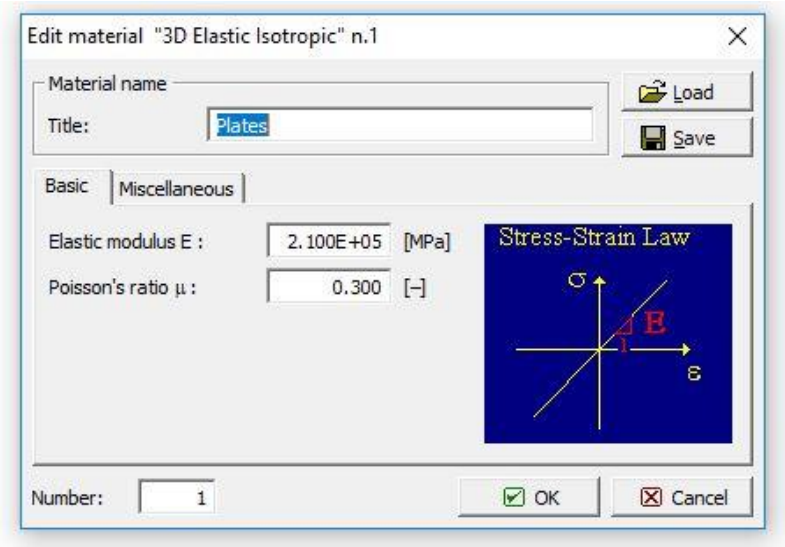

Figure 2.13 Basic Properties of Steel Plates.

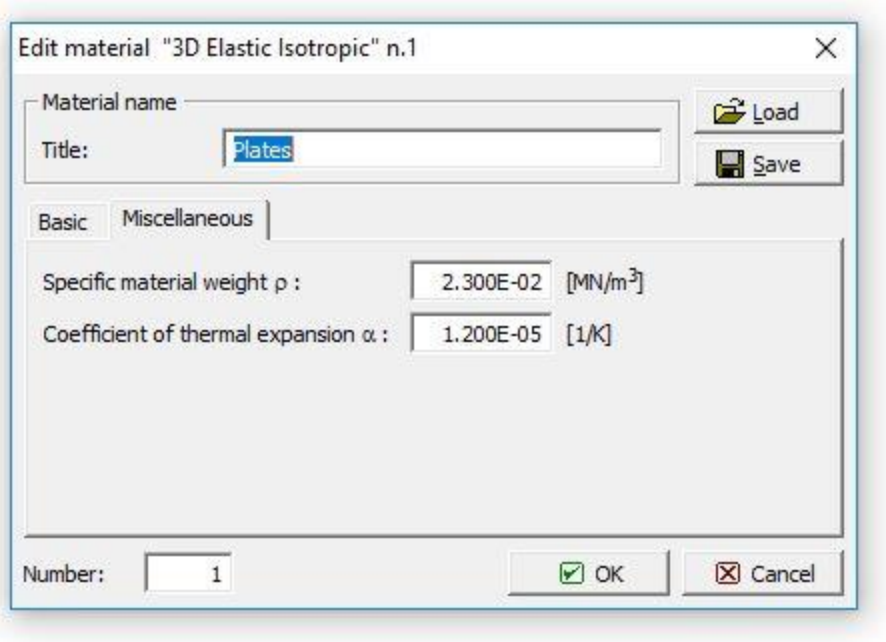

Figure 2.14 Miscellaneous Properties of Steel Plates.

Definition of Material Properties for Reinforcement

Ribbed reinforcement B500 was used in the experiments. Therefore, corresponding properties are also used as input in simulations.

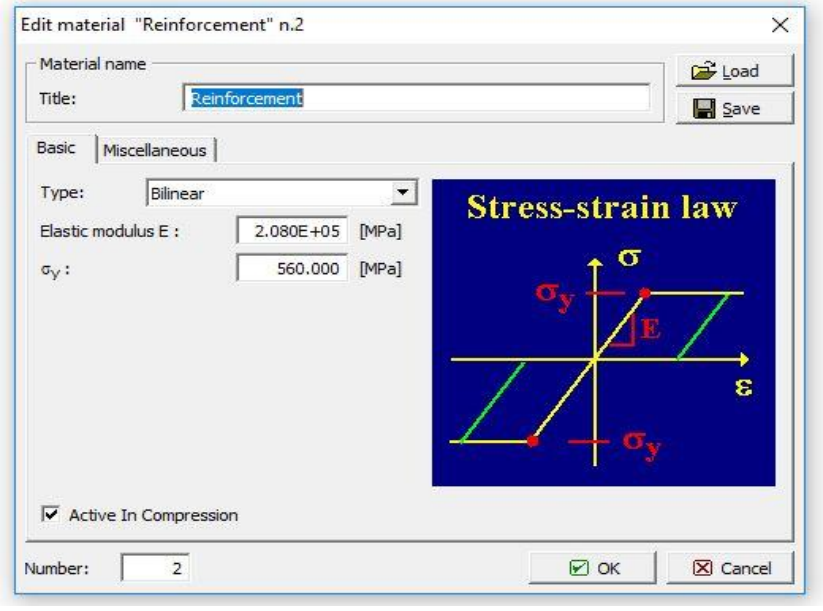

Figure 2.15 Basic Properties of Steel Reinforcement.

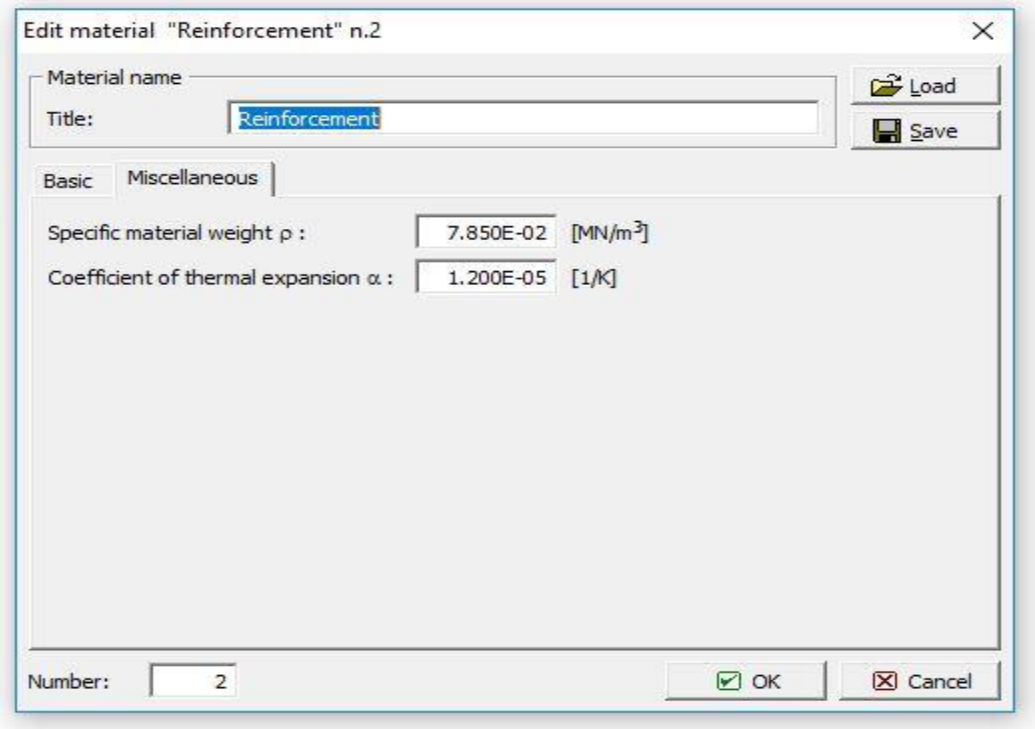

Figure 2.16 Miscellaneous Properties of Steel Plates.

The next step is to define the loading/support conditions and then the mesh properties. In this research a mesh size of 30mm is chosen. Later the mesh refinement is also studied for its effect on the results. The geometry of model along with the mesh is shown in Figure 2.17.

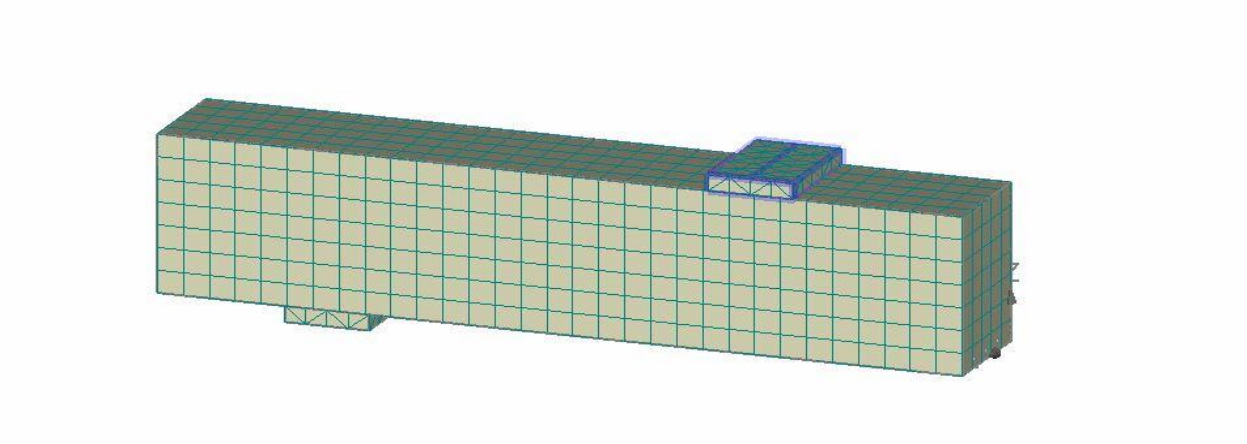

Figure 2.17 ATENA modelling showing geometry of the beam and mesh.

2.3.1 Modelling of the SHCC Layer.

To model the tensile hardening behavior of SHCC material a user defined tension curve is used. Since the SHCC layer shows an increase in ultimate tensile stress after the first cracking the behavior of SHCC in tension is defined according to the curve in Figure 2.18.

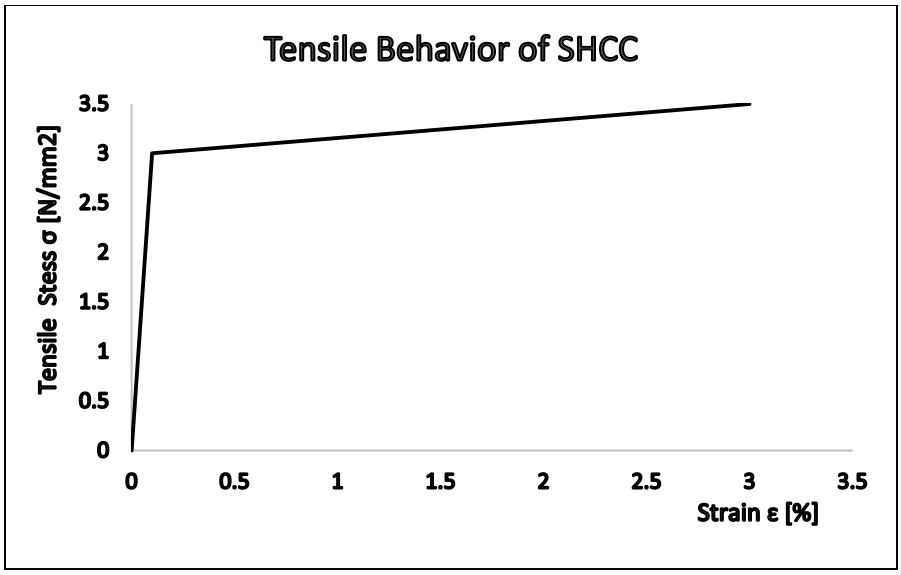

Figure 2.18 Tensile Curve of SHCC.

The above curve is modelled in ATENA using the user defined material. This is shown in the figures.

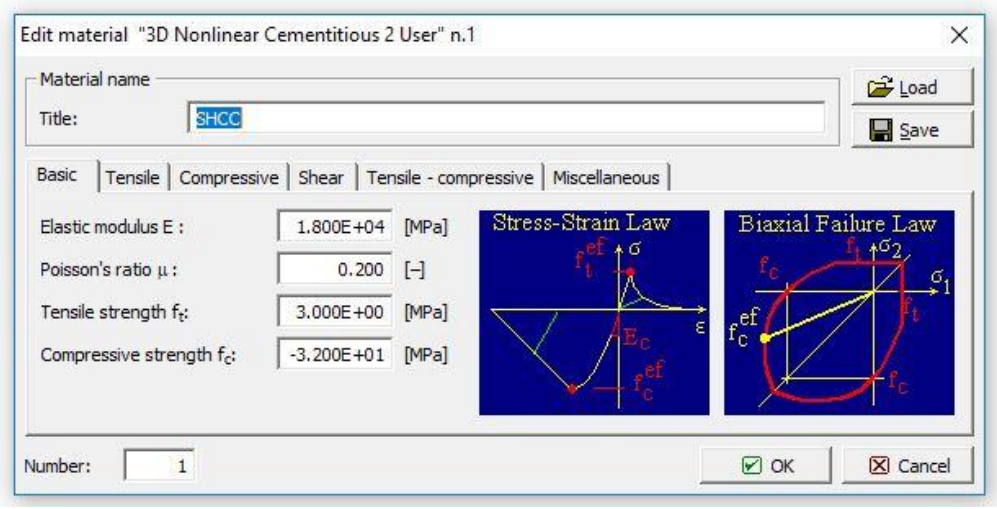

Figure 2.19 Basic Properties of SHCC.

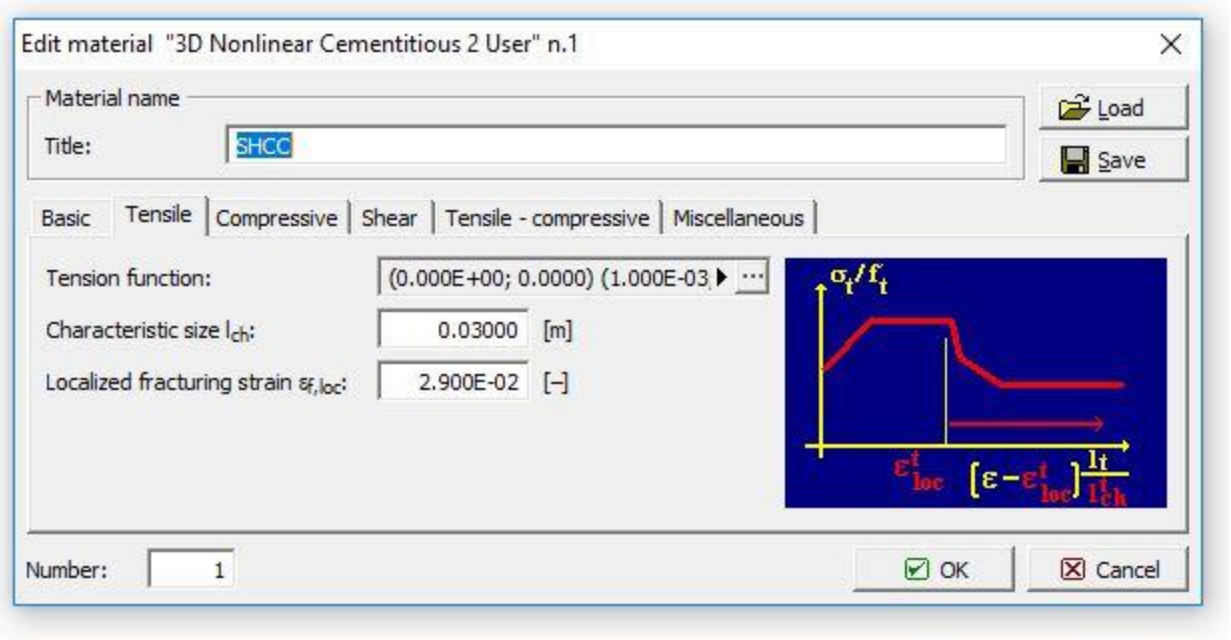

Figure 2.20 Basic Properties of SHCC

.

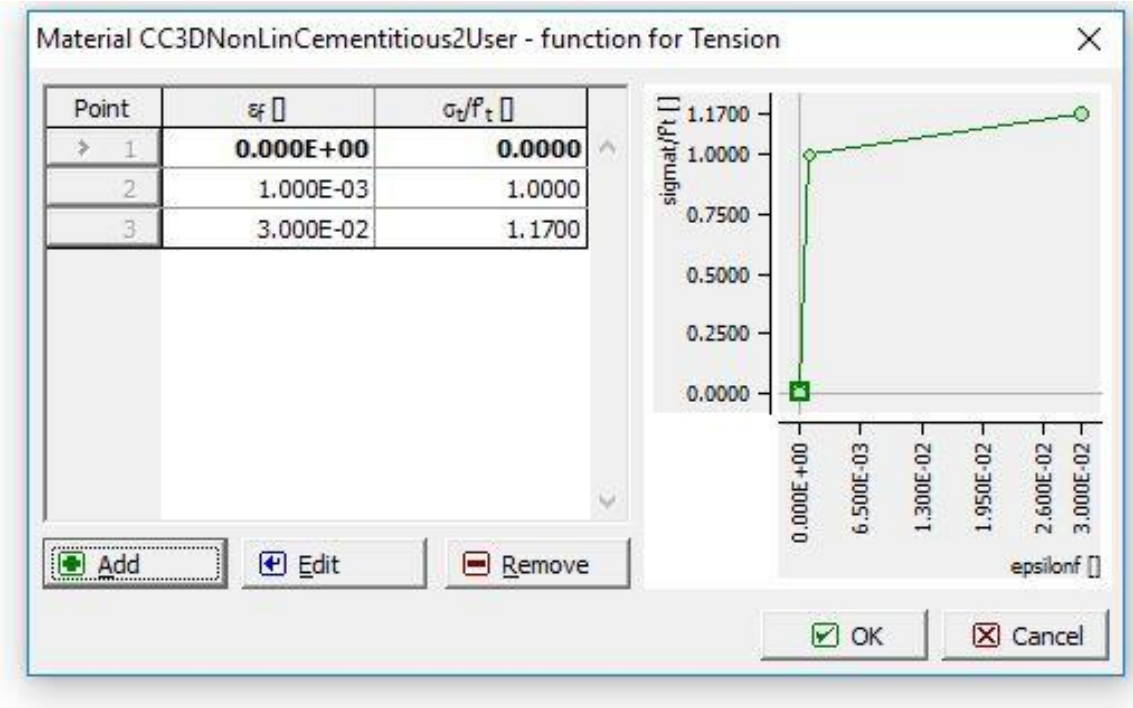

Figure 2.21 Tensile Function of SHCC material.

Prior to performing the simulations, the solution parameters such as the solution method, required number of iterations/steps, increments for each iteration had to be specified. It is also possible to define specific points in the model for monitoring the results in a particular node/point. All the above mentioned steps are carried out in the pre-processor tab.

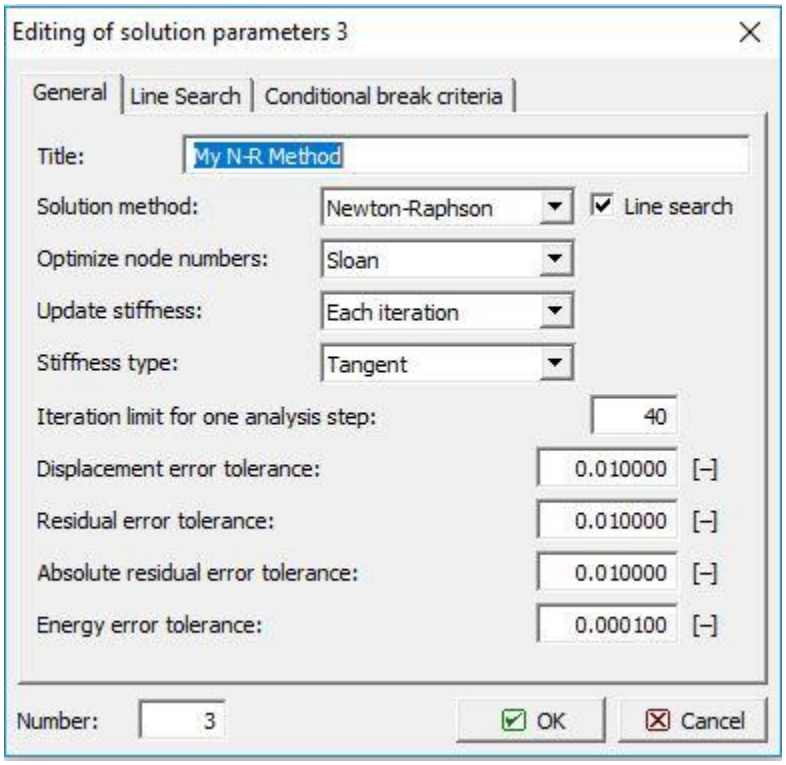

Figure 2.22 Definition of Solution methods and Parameters.

Once the mesh is generated, the analysis can be carried out. After the computation is finished, the results can be viewed in post-processor window.

3 Experimental Procedure

The beams are modelled using ATENA Programme and are subjected to 4 point bending test. Displacement control method is used during the experimental and numerical testing. The total displacement is applied in steps with increments after each step (0.015mm each step). In the experiment, displacement speed of loading jack was 0.01 mm/sec.

In the numerical simulation, in order to ensure the failure of the beam a total displacement of 6mm (40 steps with 0.015 increment) are defined.

Due to symmetry in beam length and symmetric loading conditions only half of the beam is modelled in ATENA and analyzed to avoid excessive computation time. Therefore the load at failure determined using simulation is equal to half the load capacity obtained from the actual experiment.

The dimensions of the beams are in accordance with the experimental model of Mr. Zhekang Huang, a Master's student conducting an experimental research on the same topic for his graduation thesis. This gave an opportunity to compare the results from the numerical analysis with that of the experiment.

The ATENA model of the beams is shown in Figure 3.2 to Figure 3.5. In order to satisfy the symmetric condition the right hand side of the beam is fixed in the horizontal direction. Steel plates are used for both loading and support to avoid unrealistic stress concentration which may affect the analysis results.

The results are monitored with 4 points

1. Deflection at Mid-span.
2. Load at Failure.
3. Horizontal displacement at the side of the beam, in the middle of SHCC layer.
4. Horizontal displacement at a point just above the SHCC layer.
5. Horizontal displacement at 2 points the bottom surface of the beam.

The positions of the monitoring points are identical to locations of Linear Variable Differential Transformers (LVDT) in the experimental set up. These points are shown in Figure 3.1. The points marked 2, 3, 4, 7 & 10 are used in the simulation. (1 is the deflection at mid-point of the beam.)

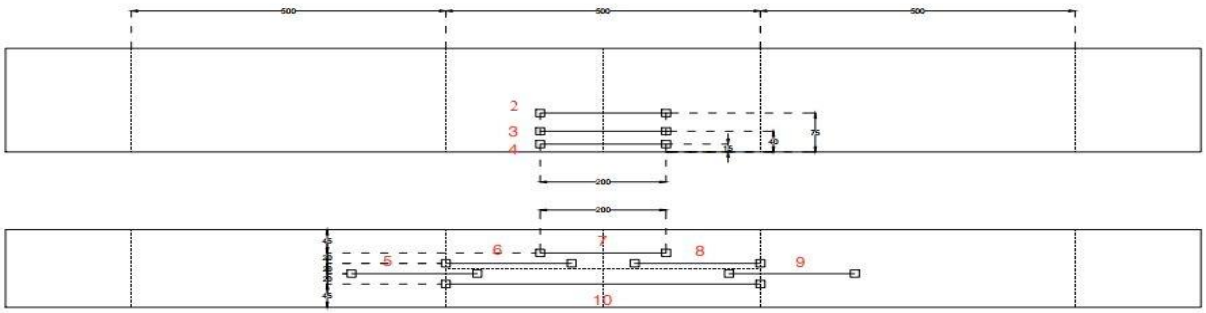

Figure 3.1 Position of monitoring points used in the experimental set up.

3.1 Models in ATENA.

The models used for simulation of beams are prepared in ATENA. A mesh of size of 30 mm is used. Later finer meshes are made to study the effect of mesh refinement on the results of the analysis.

The models used for analysis, with different concrete and SHCC cover are shown in the figures below.

The results, such as the plot of load vs Deflection and crack patterns, are obtained in the post- processor of ATENA.

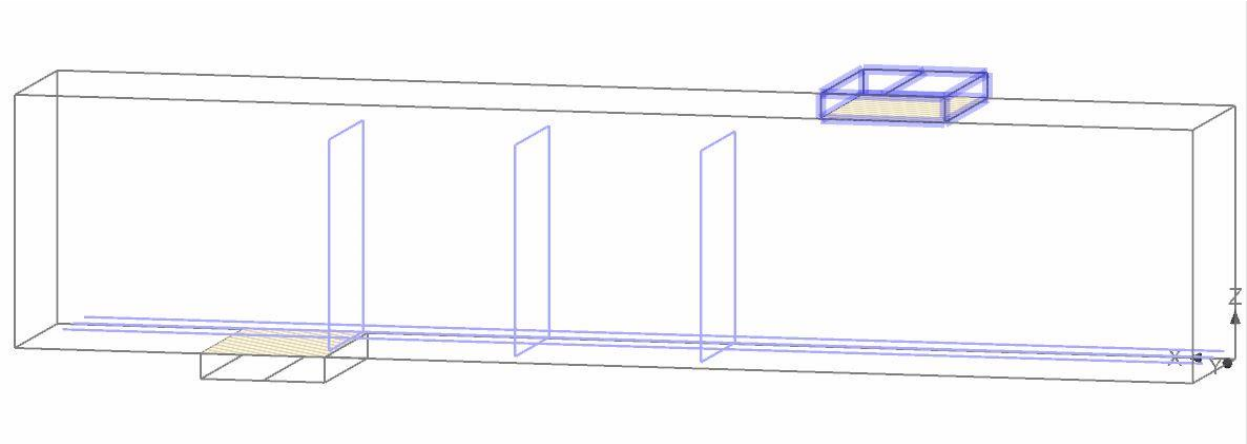

Figure 3.2 ATENA model of Reinforced Concrete Beam with 11mm Reinforcement cover.

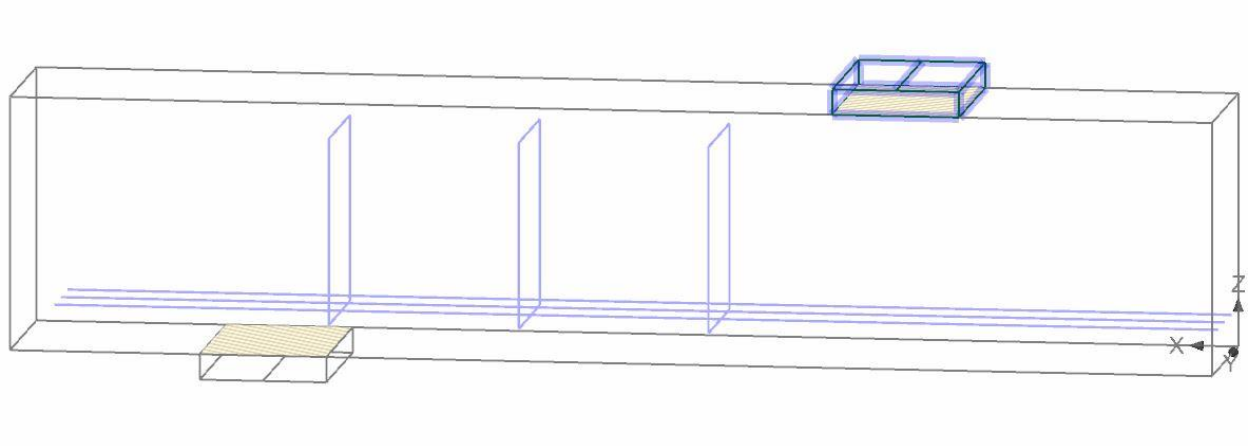

Figure 3.3 ATENA model of Reinforced Concrete Beam with 31mm Reinforcement cover.

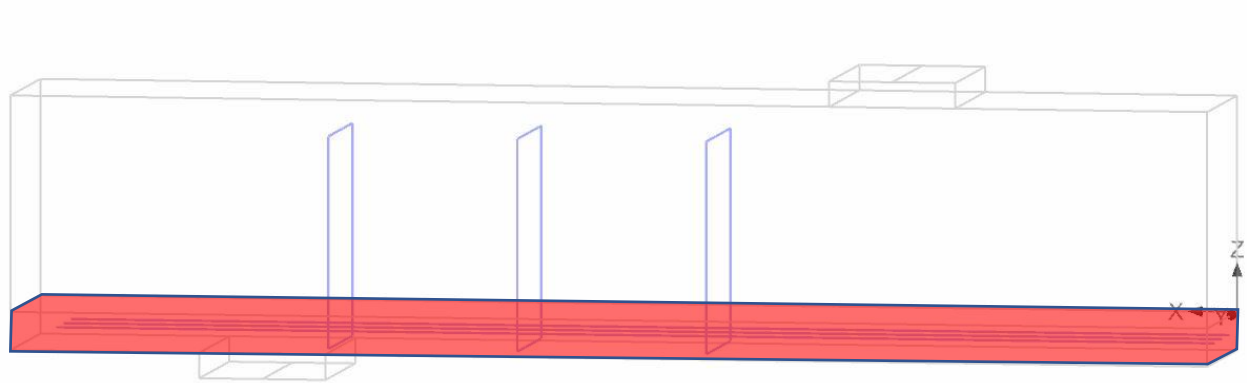

Figure 3.4 ATENA model of Reinforced Concrete Beam with 31mm SHCC layer in the tension zone (marked in red) and 11mm reinforcement cover.

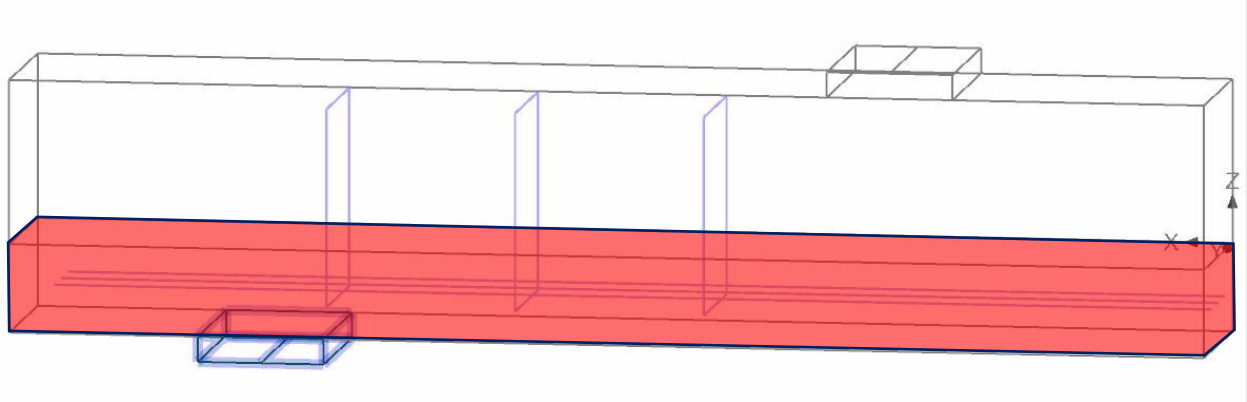

Figure 3.5 ATENA model of Reinforced Concrete Beam with 70mm SHCC layer in the tension zone (marked in red) and 31mm reinforcement cover.

4 RESULTS.

4.1 Results of ATENA.

The results of analysis from ATENA (**using a mesh of 30mm size**) are obtained in post-processing tab. In this research we are concerned with the load at fracture of the beams and also the crack pattern and information about the crack width and crack spacing.
The failure load can be obtained from the Load vs Deflection graph. This can be seen in the figures. The development of cracks (marked with dashed line in Figure 4.1.) is shown for every 5kN load interval (Figure 4.2). A minimum crack width of 50 micron is chosen for display. The same approach is used for presenting the analysis results of all the beams.

4.1.1 Reinforced Concrete Beam with 11mm Reinforcement Cover.

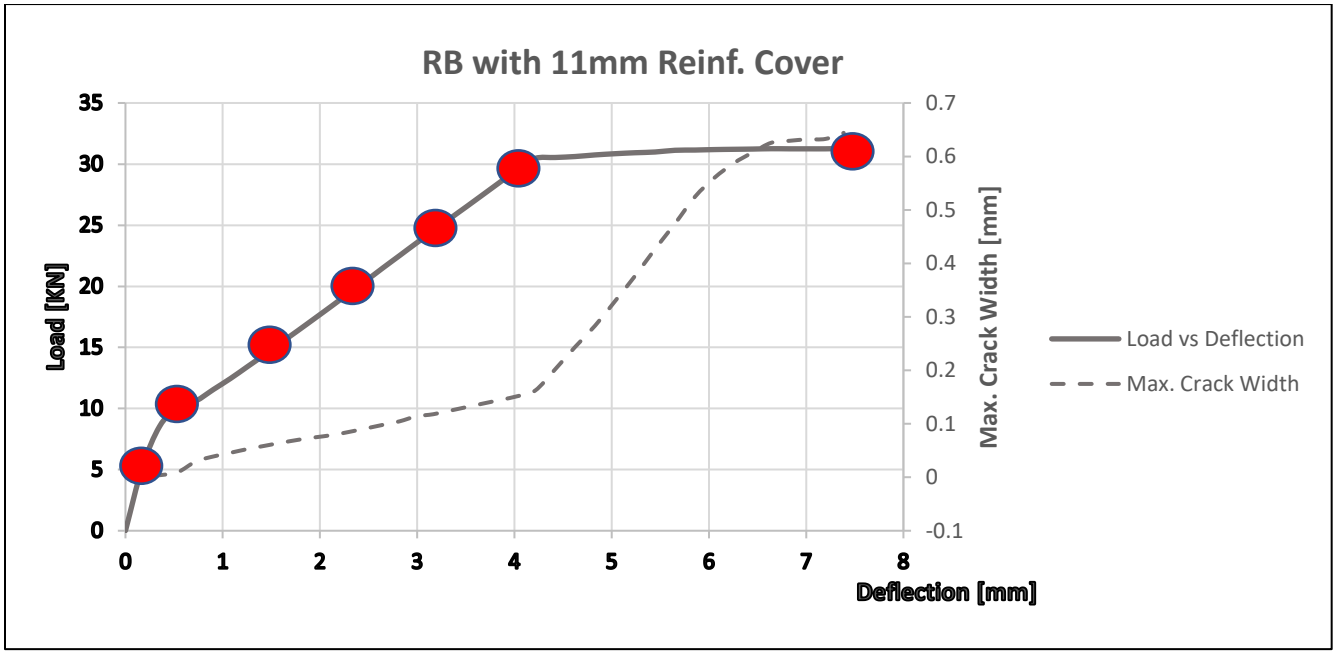

Figure 4.1 Load vs Deflection vs Max. Crack Width Plot for RB with 11mm cover.

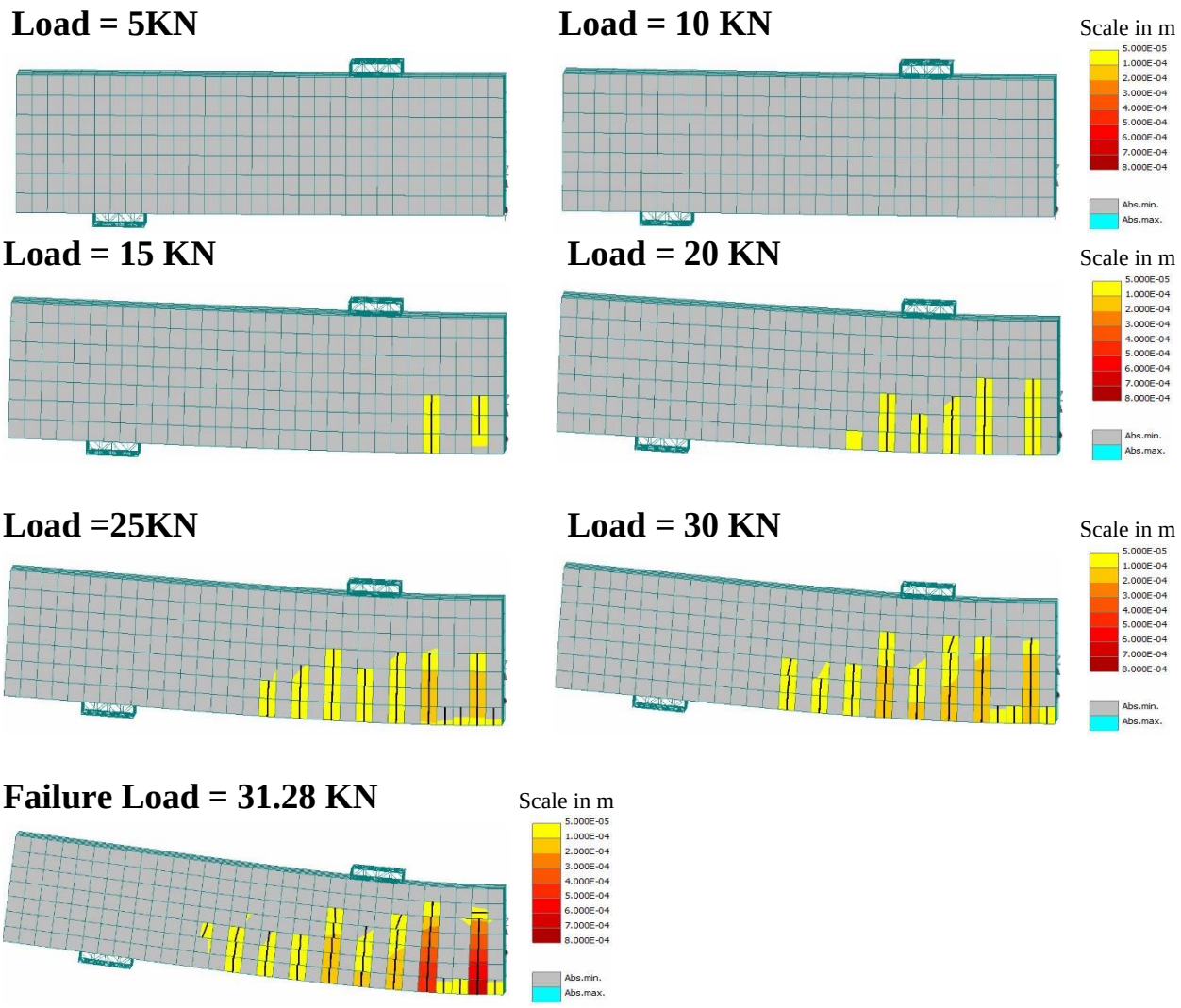

Figure 4.2 Crack Development in RB with 11mm Reinforcement Cover.

4.1.2 Reinforced Concrete Beam with 31mm Reinforcement Cover.

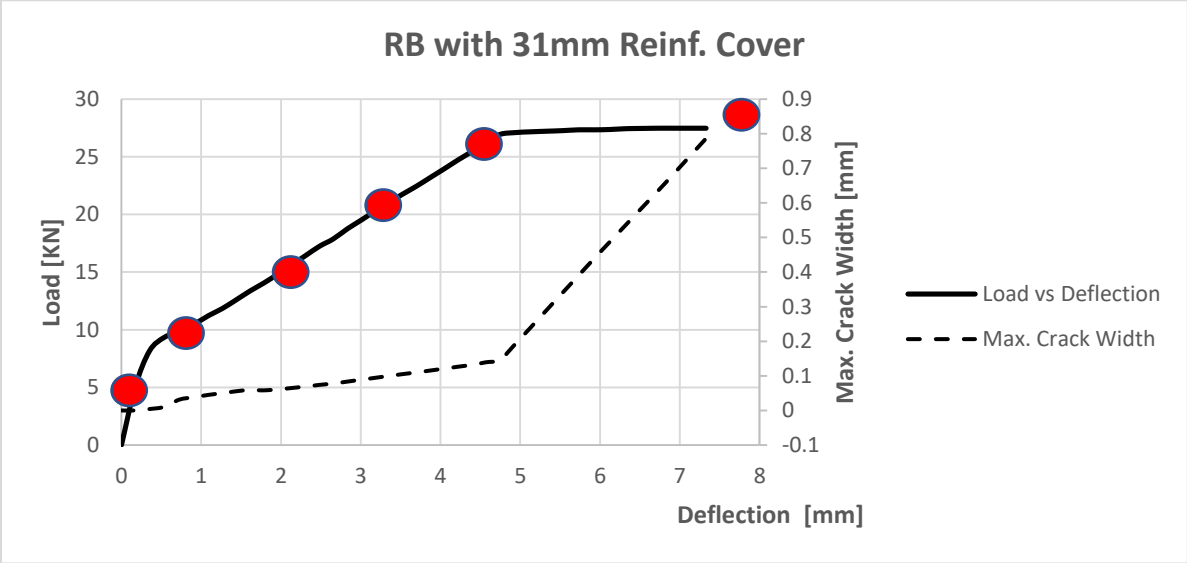

Figure 4.3 Load vs Deflection vs Max. Crack Width Plot for RB with 31mm Reinforcement cover.

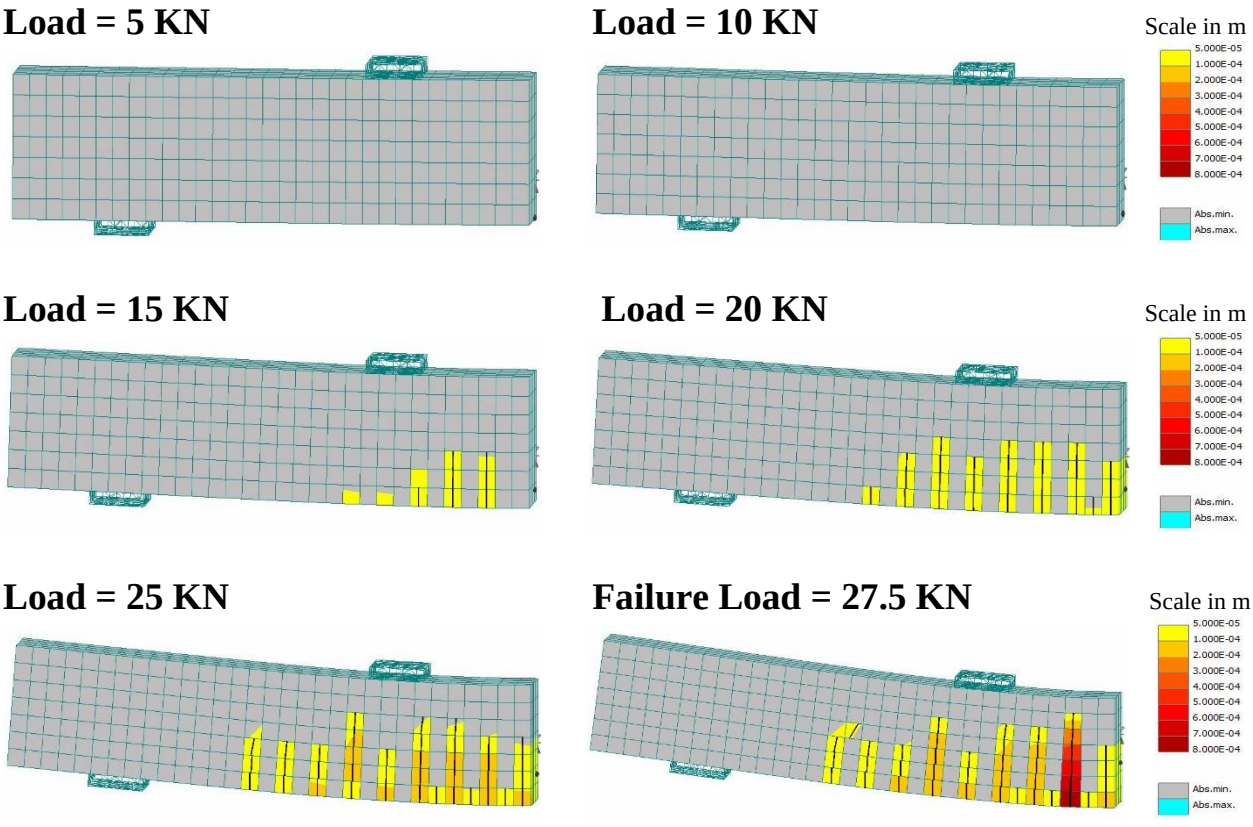

Figure 4.4 Crack Development in RB with 31mm Reinforcement Cover.

4.1.3 Reinforced Concrete Beam with 31mm SHCC Cover.

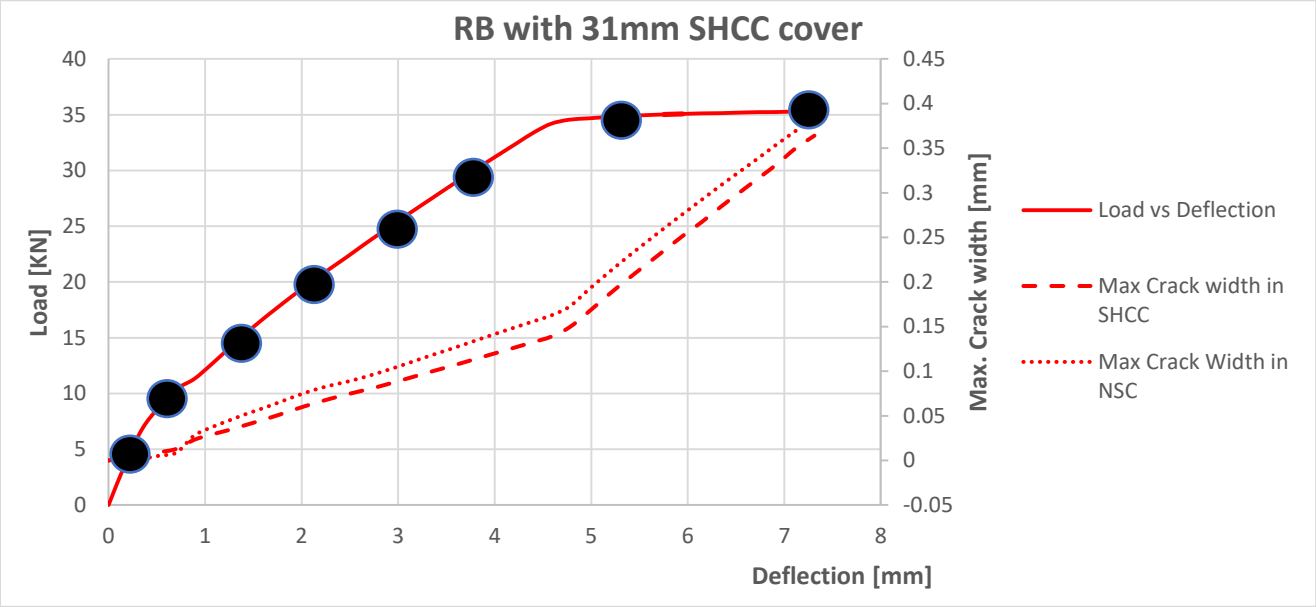

Figure 4.5 Load vs Deflection vs Max. Crack Width Plot for RB with 31mm SHCC cover.

Load = 5 KN

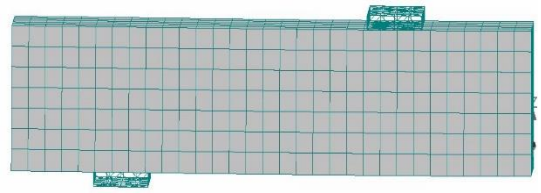

Load = 10 KN

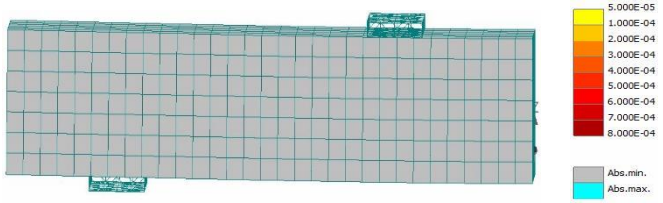

Load = 15 KN

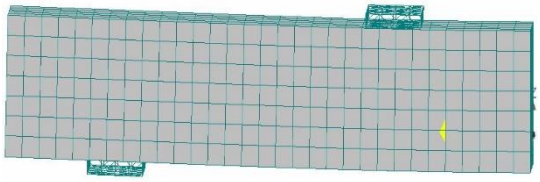

Load =20 KN

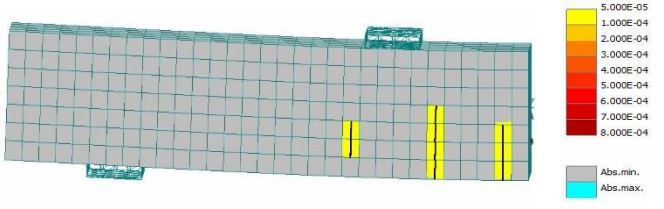

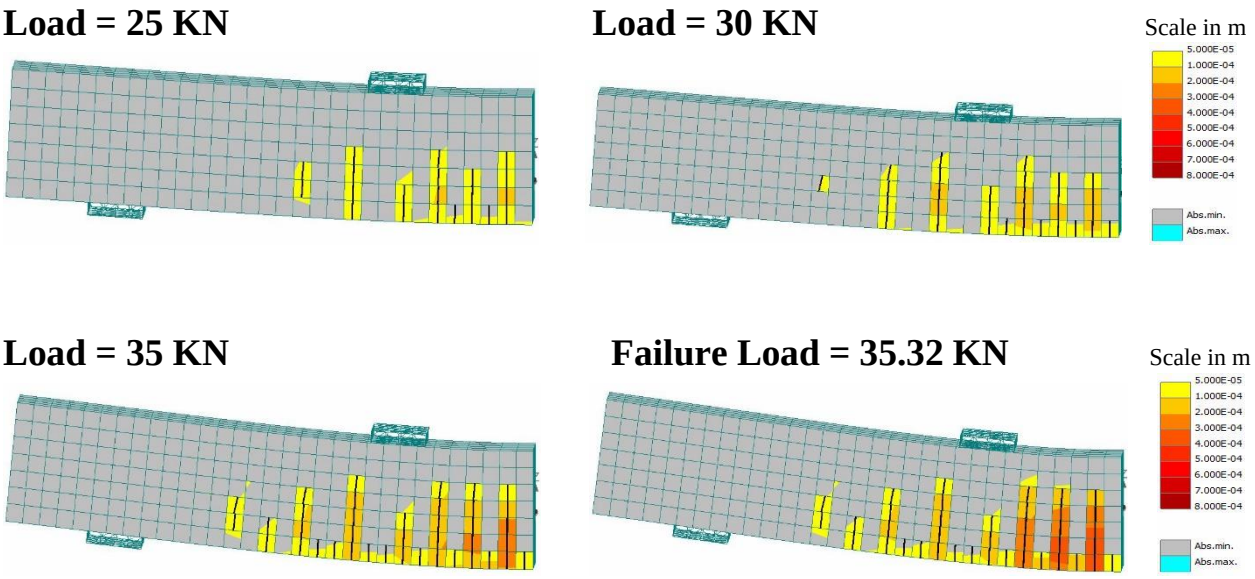

Figure 4.6 Crack Development in RB with 31mm SHCC Cover.

4.1.4 Reinforced Concrete Beam with 70mm SHCC Cover.

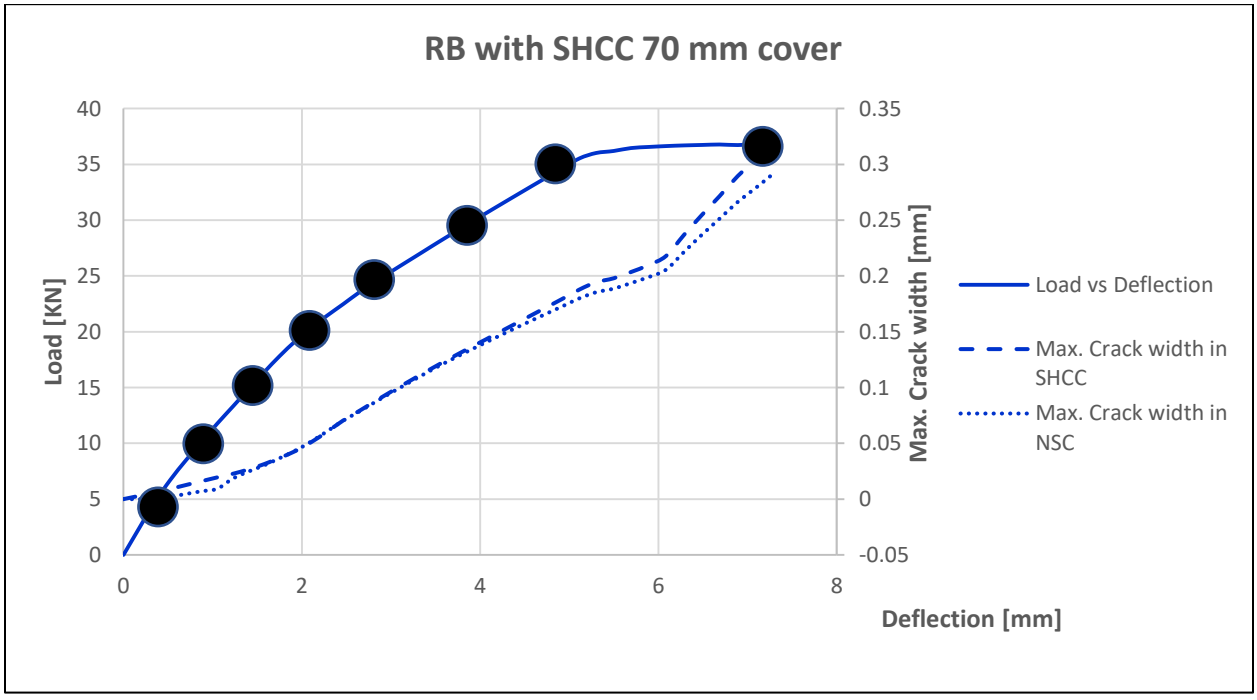

Figure 4.7 Load vs Deflection vs Max. Crack Width Plot for RB with 70mm SHCC cover.

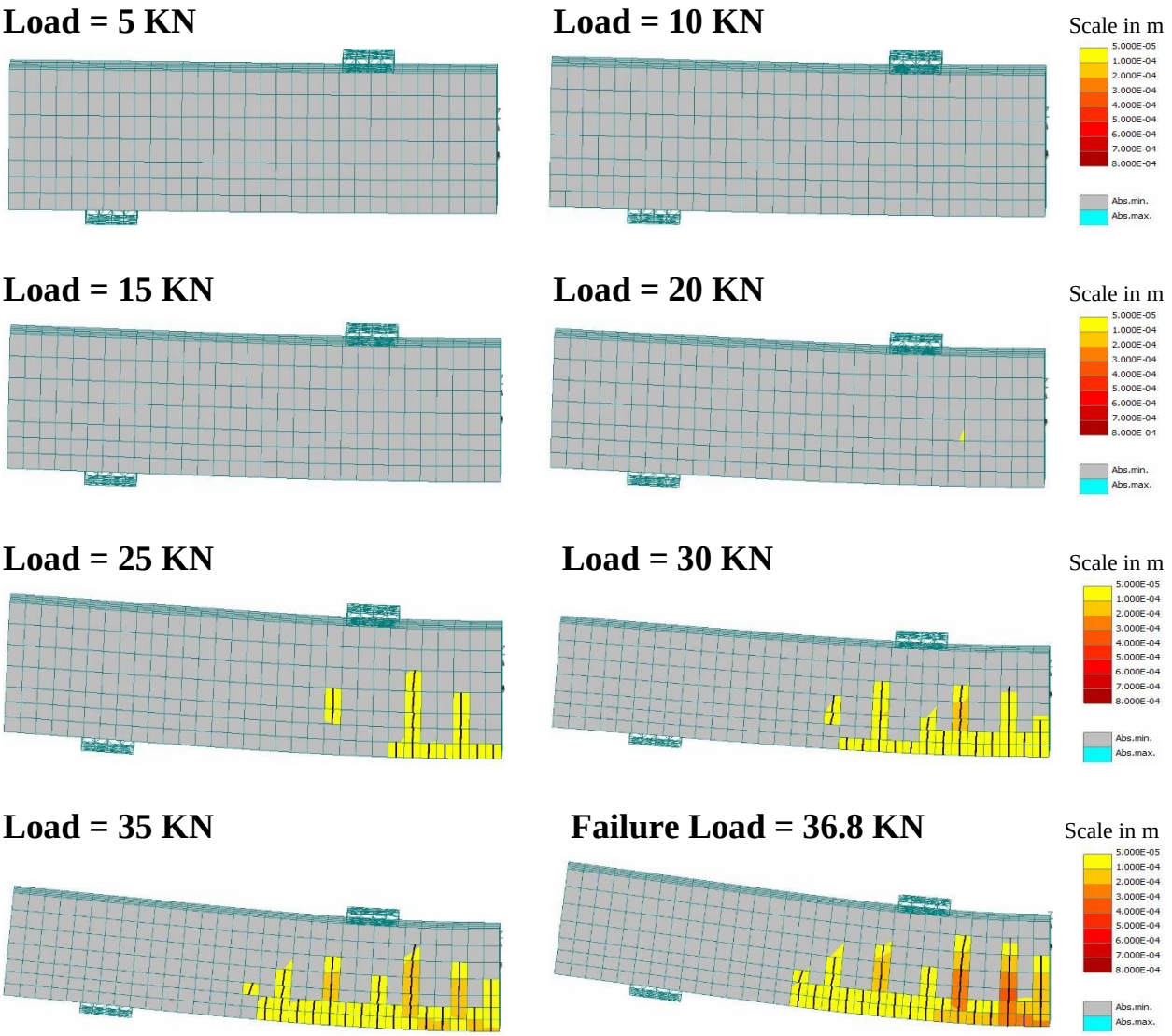

Figure 4.8 Crack Development in RB with 70mm SHCC Cover.

The results obtained from all the analyses are tabulated in the table shown below.

Table 4-1 Results obtained from Simulation in ATENA

Beam	Failure Load (KN)	Failure Load from Experiment (KN)	Max. Crack Width at yielding of reinforcement (mm)	Max. Crack Width at Failure (mm)
RB with 11mm Reinforcement Cover	31.28	31.3	0.16	0.644
RB with 31mm Reinforcement Cover	27.5	29	0.14	0.786
RB with 31mm SHCC cover	35.3	34.7	0.17	0.384
RB with 70mm SHCC cover	36.8	35.5	0.19	0.32

Note: The computation of crack widths under failure for experiment is still under progress by Mr. Zhekang Huang

4.2 Comparison between NSC Beams and Beams with SHCC in the tension Zone.

The main purpose of this research was to determine the benefits of having an SHCC layer in the tension zone of Reinforced beams. In order to do this a comparison has to be made between NSC beams and NSC beams with the reinforcement embedded in the SHCC layer having similar reinforcement cover.

Two different comparisons are made.

1. NSC beam with 11 cover Reinforcement cover and NSC-SHCC beam with 11 mm cover and 31mm SHCC layer in the tension Zone.
2. NSC beam with 31 cover Reinforcement cover and NSC-SHCC beam with 31 mm cover and 70 mm SHCC layer in the tension Zone.

By comparing the failure load, crack pattern, maximum crack width in the above mentioned comparisons, the possible benefits of embedding reinforcements in the SHCC layer can be identified.

4.2.1 NSC beam with 11 cover Reinforcement cover and NSC-SHCC beam with 31mm SHCC layer in the tension Zone.

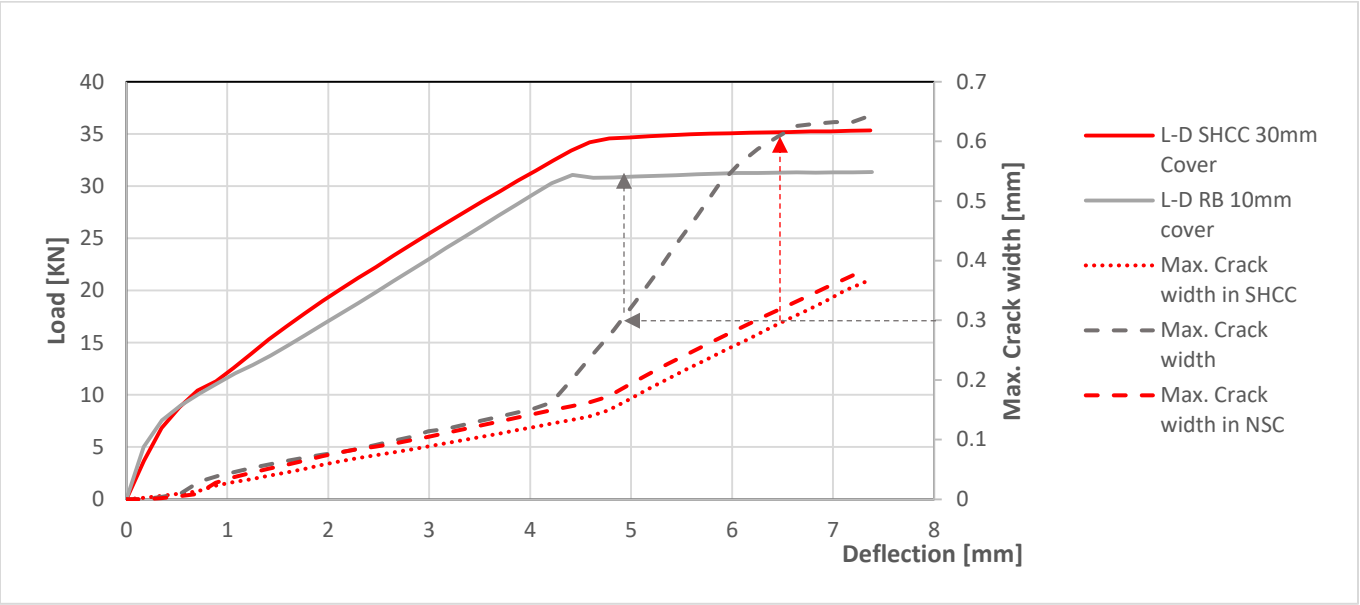

Figure 4.9 Load vs Deflection vs Max. Crack width Curve for RB with 11 cover and RB with 31mm SHCC layer.

From the above figure it is clear that the bending load capacity of the beam with 31mm SHCC cover is much higher than that of beam with 11mm reinforcement cover. This is due to the ductile behavior and strain hardening property of SHCC in the tension zone of the reinforced beam.

In order to compare the 2 beams with respect to their crack patterns at the moment of failure, the previously seen figures are presented again.

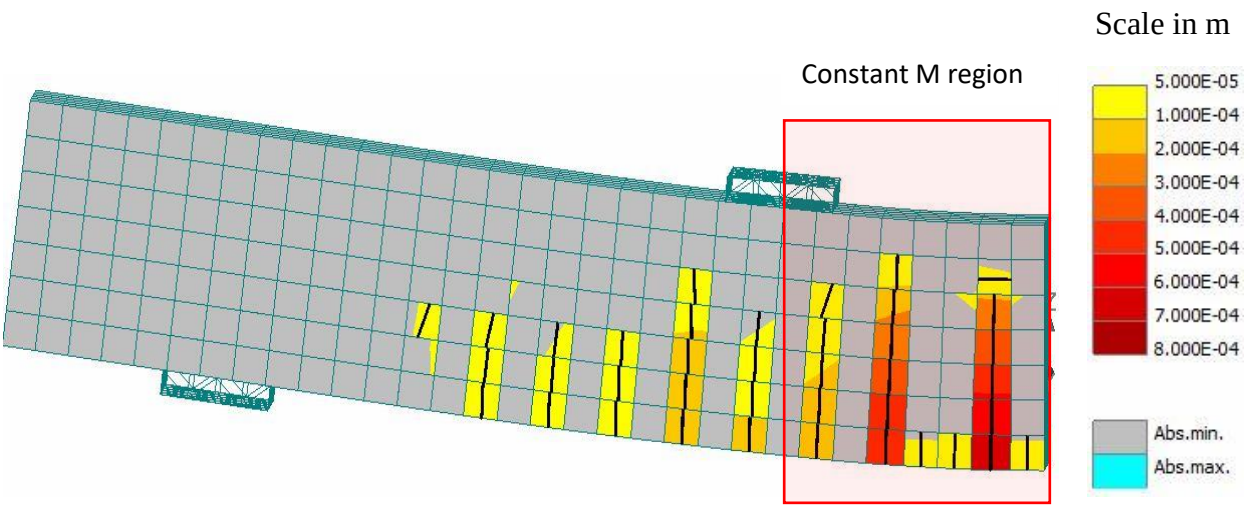

Figure 4.10 Crack pattern of RB with 11mm Reinforcement Cover at failure load (31.28KN).

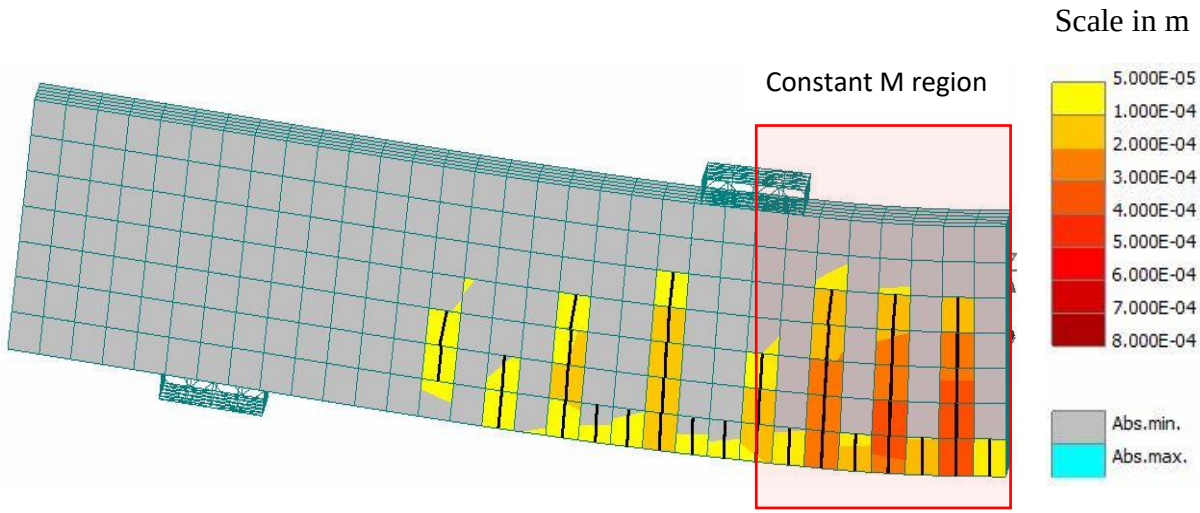

Figure 4.11 Crack pattern of RB with 31mm SHCC Cover at failure load (35.3KN).

From the figures it can be seen that there is more localization of cracks in the beam without SHCC. Two cracks with the crack width of 0.6mm can be seen in the region of constant bending moment at the failure in NSC concrete beam. The deformation is concentrated in a less number of cracks and this leads to cracks of larger width.

In the beam with SHCC in the tension zone, more cracks can be seen in the constant moment region. The width of the largest crack is about 0.4mm at the failure which

is less than in the case of the beam without SHCC in the tension zone. The crack spacing between the cracks is also smaller which is indicates a denser crack pattern.

Although there is a difference of crack widths at the failure, this difference is obvious only after yielding of the reinforcement. Before the yielding, under the same loading, there seems to be no difference in crack widths between the two beams.

Therefore, by comparing the crack widths between the beams, there seems not to be difference, at least not for the beam with the perfect bond between the concrete and the reinforcement, and with this amount of reinforcement. However by comparing the failure load of the two beams, the benefits of having an SHCC layer in the tension zone is fairly obvious.

Now the cover thickness is varied and a similar comparison is made.

4.2.2 NSC beam with 31 cover Reinforcement cover and NSC beam with 70 mm SHCC layer in the tension Zone.

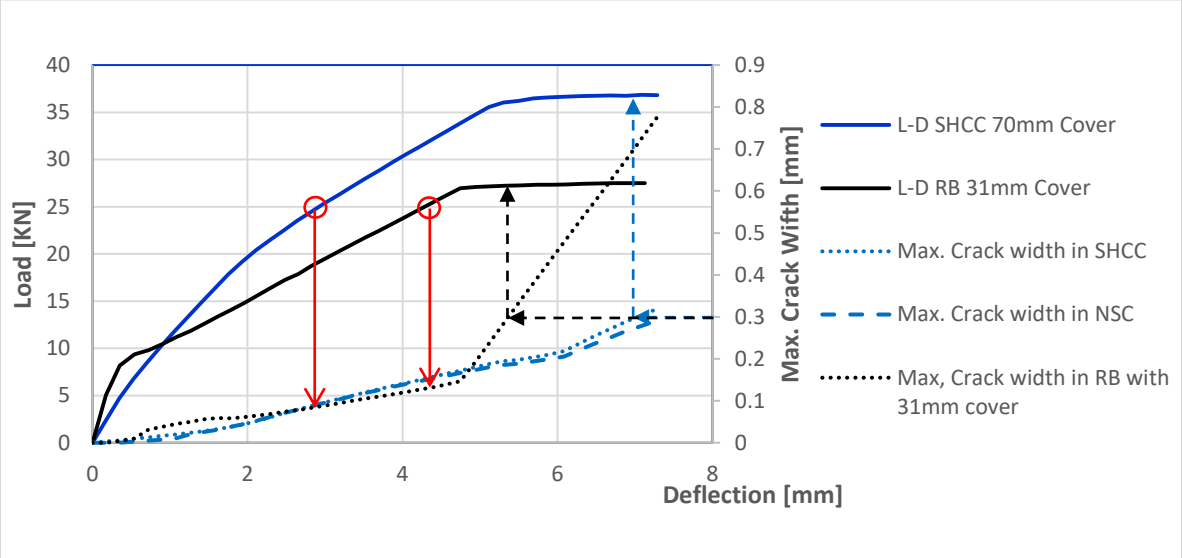

Figure 4.12 Load vs Deflection vs Max. Crack width Curve for RB with 31 cover and RB with 70mm SHCC layer.

Similar to the earlier comparison, the beam with reinforcement embedded in the SHCC has a higher load capacity (36.8KN) compared to the one without SHCC.

The RB which has a cover of 31mm has the lowest load capacity (27.5KN) of the four beams analyzed. This is due to the reduction of internal lever arm with a reinforcement cover of 31mm.

By comparing the crack patterns of the two beams it can be observed that similar to the previous comparison, the beam without SHCC shows a crack pattern with localization of a single crack in the region of constant bending moment. In the beam with SHCC in the tension, more micro cracking can be seen and the crack width is distributed among many cracks preventing formation of large cracks. The maximum crack width here is as low as 0.3mm at the failure. Also it can be observed that the crack width is larger in the concrete than at the SHCC zone meaning that one large crack in concrete is smeared over more cracks in SHCC.

Also there seems to be some crack width difference in the two beams. For example at the load of 25 kN, the maximum crack width in SHCC beam is around 0.09mm while in NSC beam is around 0.13mm.

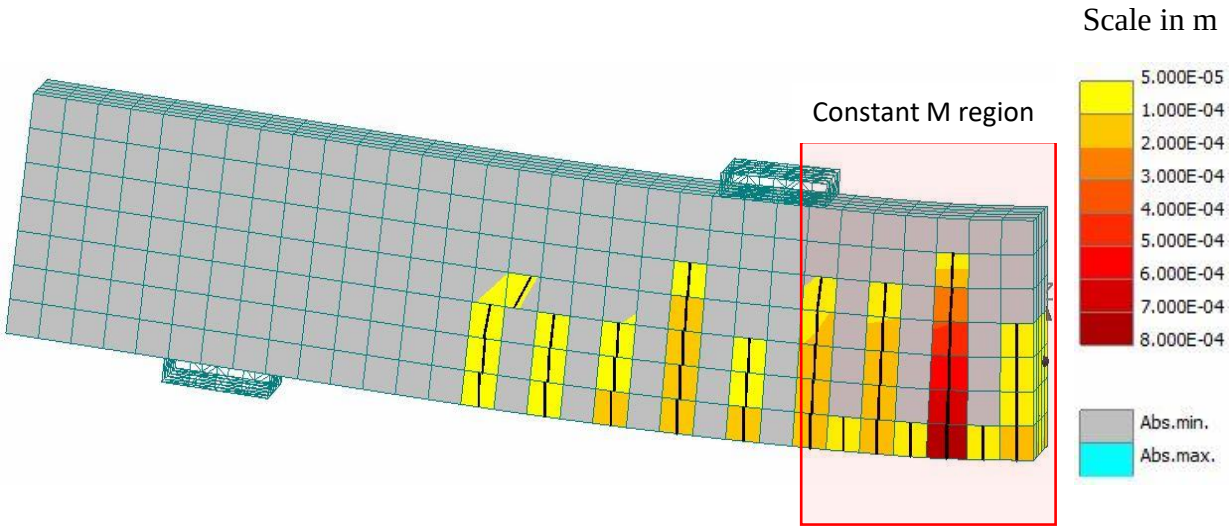

Figure 4.13 Crack pattern of RB with 31mm Reinforcement Cover at failure load (27.5KN).

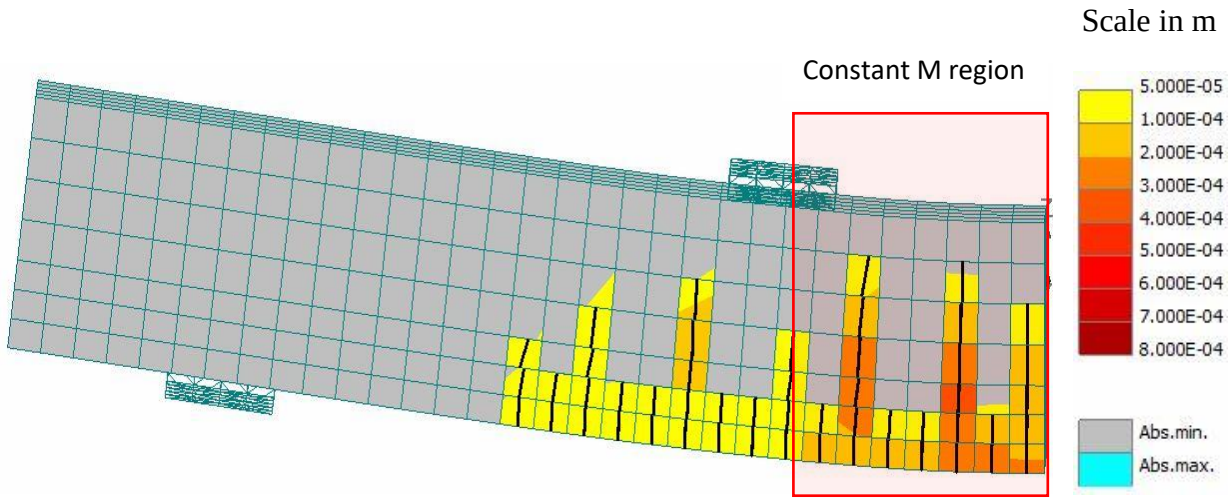

Figure 4.14 Crack pattern of RB with 70mm SHCC Cover at failure load (36.8KN).

4.3 Comparison of Numerical and Experimental Results.

The results obtained from the numerical simulation and the experiments performed by Mr. Zhekang Huang are compared to verify the accuracy of the results and check for possible deviations and discrepancies.

First the Load vs Deflection curves are compared. Since the experiments were carried out with a full length beam and the simulations consisted of only one half of the beam, only half the failure load obtained from the experiments are used in the comparison.

4.3.1 Reinforced Beam with 11mm Cover.

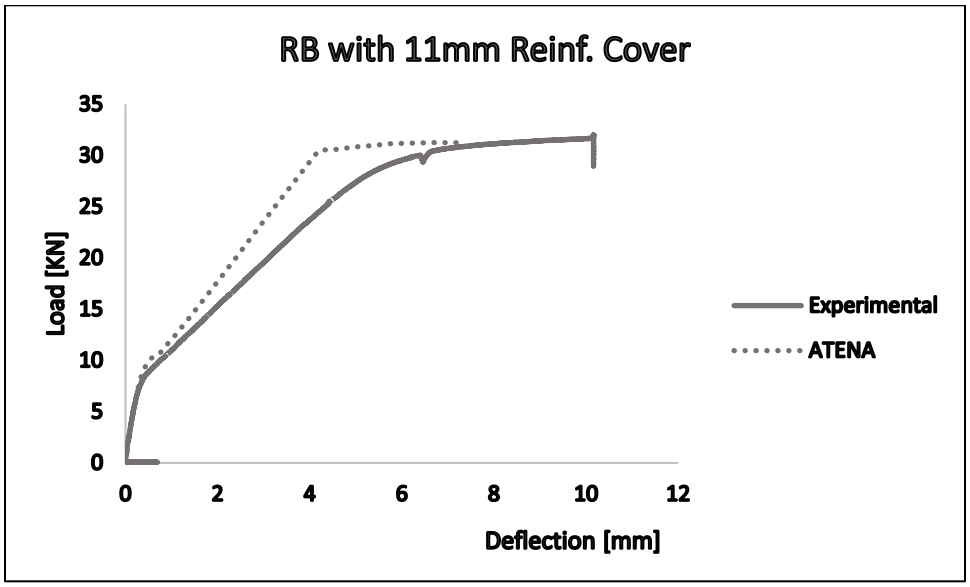

Figure 4.15 Comparison of Load vs Deflection curve for Experimental and Numerical Analysis for RB with 11mm Reinforcement Cover.

From the figure, we can see that the failure load in both the experiment and numerical analysis is similar, although the plot using ATENA shows a stiffer profile of the load – displacement relationship.

We also compare the crack patterns from numerical and experimental analysis. The crack patterns obtained from experimental analysis are presented in the form of the strain energy in the cracks obtained from Digital Image Correlation (DIC). The crack pattern at failure is compared in both the cases.

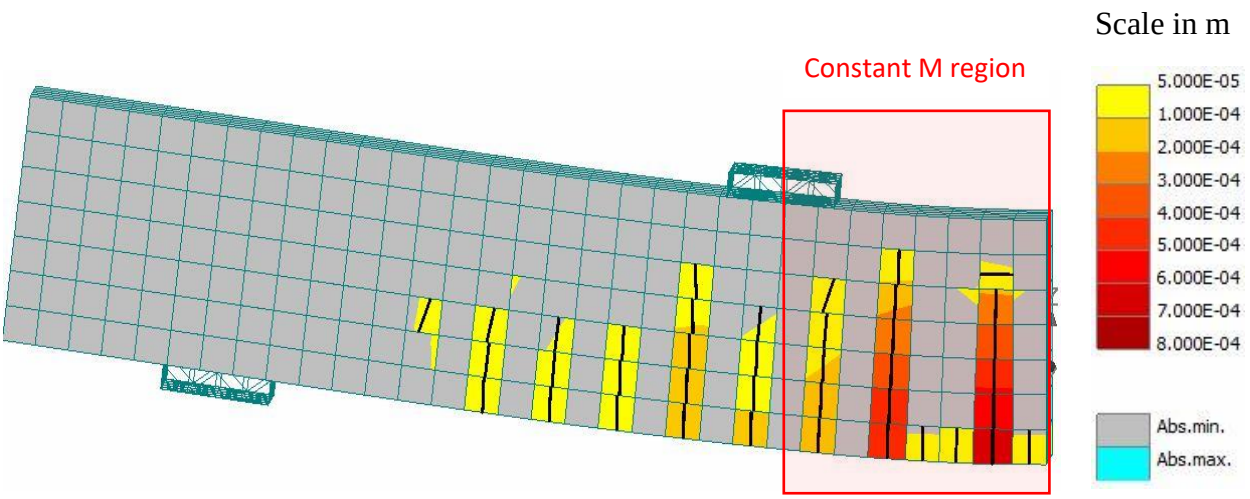

Figure 4.10 Crack pattern of RB with 11mm Reinforcement Cover at failure load (31.28KN)

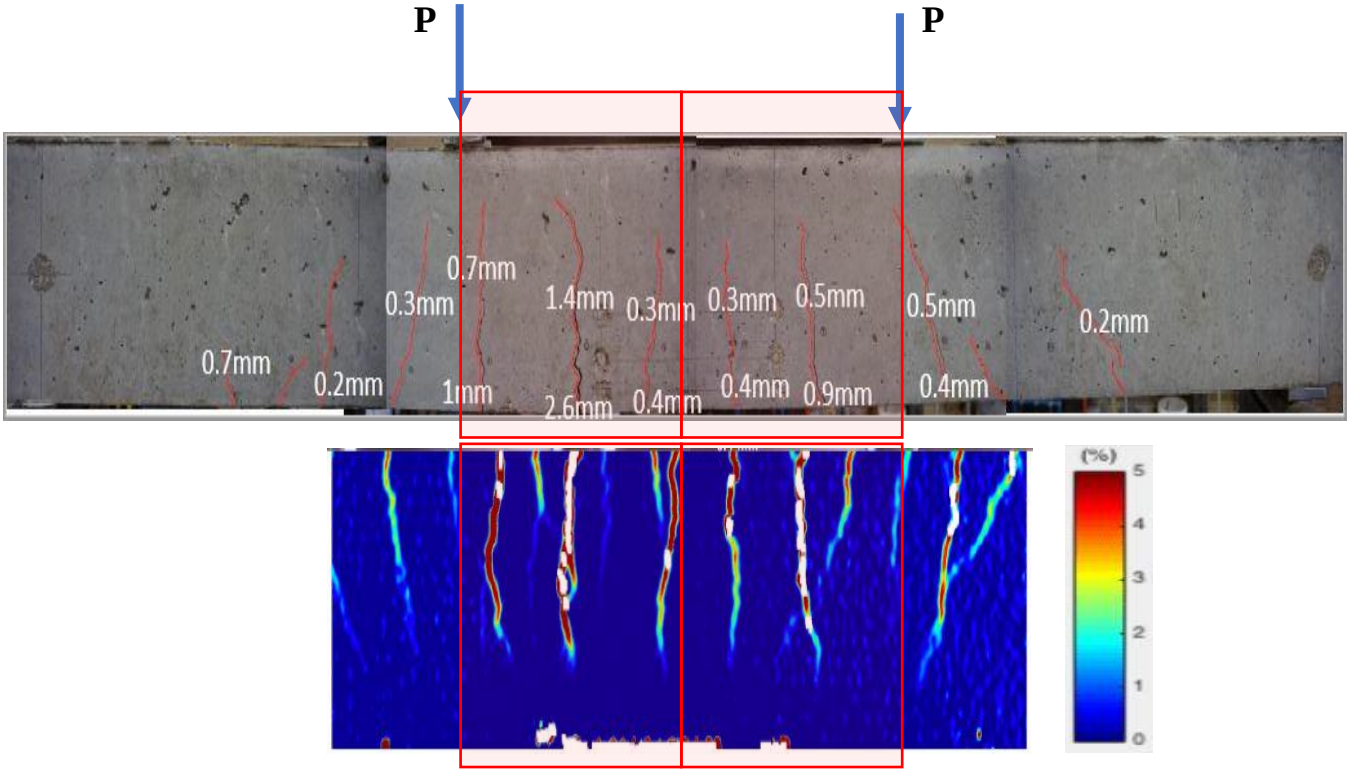

Figure 4.16 Crack Pattern & Strain Energy (εxx) in Cracks obtained from DIC Upside down) at Failure for RB with 11mm Reinforcement cover from experimental analysis

The numerical simulation shows more cracks with smaller widths than in the experiment. The maximum crack width is also larger for the experimental results (the maximum crack width at the failure in experiments is 1.4 mm, Figure 4.16 while in the simulation is around 0.6 mm, Figure 4.1).

4.3.2 Reinforced Beam with 31mm Reinforcement Cover.

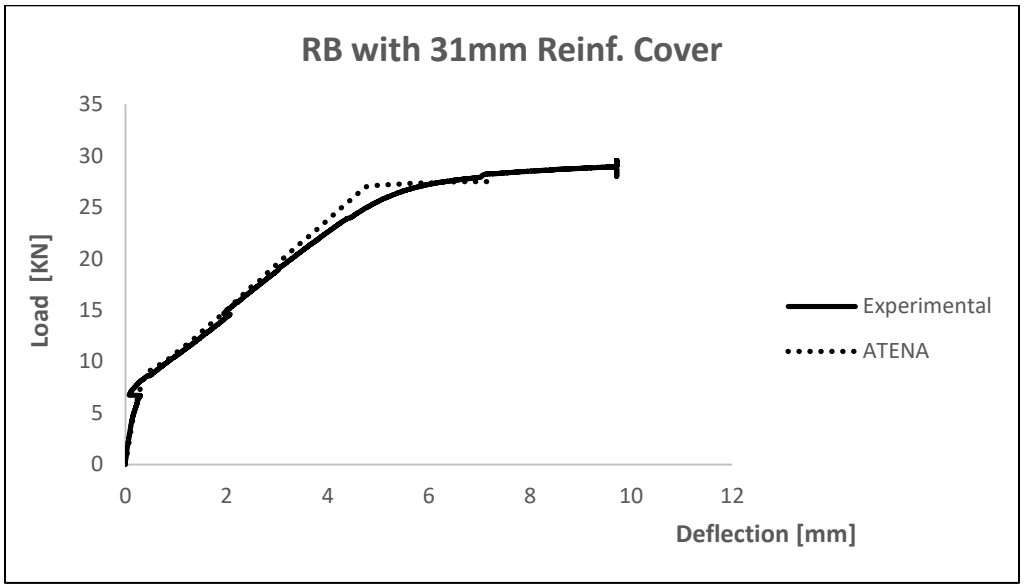

Figure 4.17 Comparison of Load vs Deflection curve for Experimental and Numerical Analysis for RB with 31mm Reinforcement Cover.

Similar to the previous comparison the Load vs Deflection relationship follow the same profile for both experimental and numerical results.

Comparing the crack patterns at failure, it can be again observed that there more cracks are observed in simulated than in the experimentally tested results. Also, the experimentally obtained maximum crack width at failure (2.1 mm) is significantly larger than the simulated one (0.8 mm)

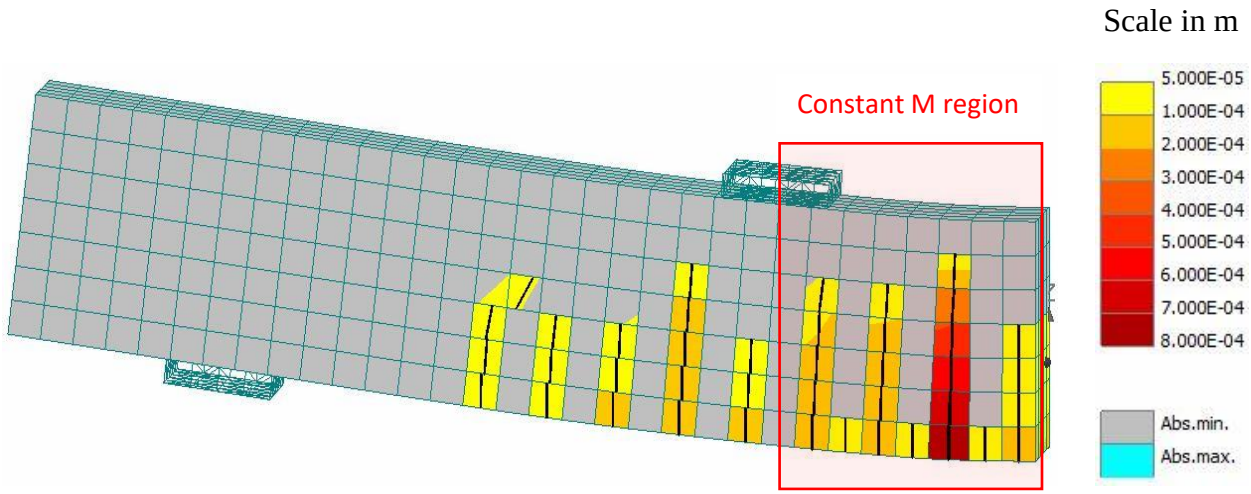

Figure 4.13 Crack pattern of RB with 31mm Reinforcement Cover at failure load (27.5KN).

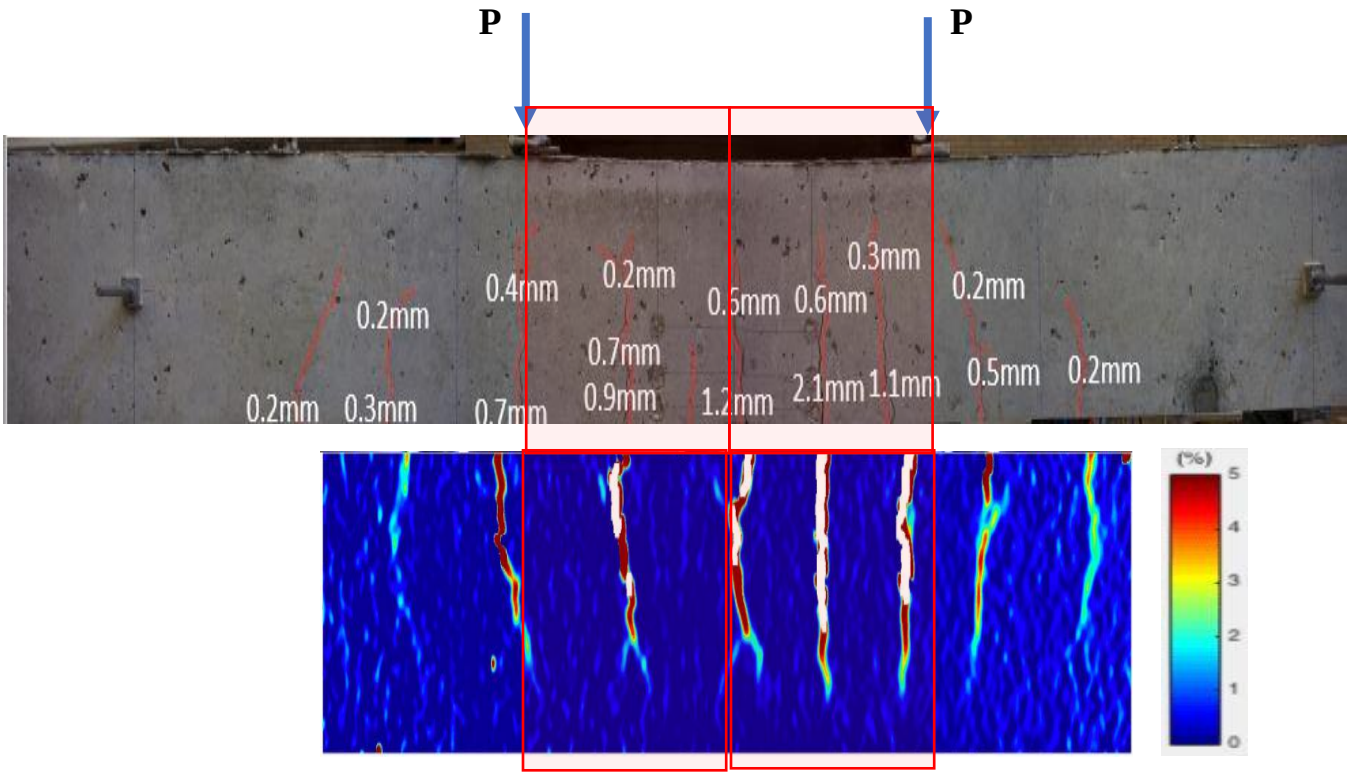

Figure 4.18 Crack Pattern & Strain Energy (εxx) in Cracks obtained from DIC at Failure for RB with 31mm Reinforcement cover from experimental analysis.

4.3.3 Reinforced Beam with 31mm SHCC Cover.

The same as with regular reinforced concrete beams, the similar comparison between the experimental and numerical results is made for the beams with the SHCC layer in the tension zone. It can be observed that in the crack formation stage, the response obtained by simulation is stiffer compared to the experimental results.

In addition, similarly as with regular concrete beams, more cracks with smaller crack widths are obtained in simulation compared to the experimental results.

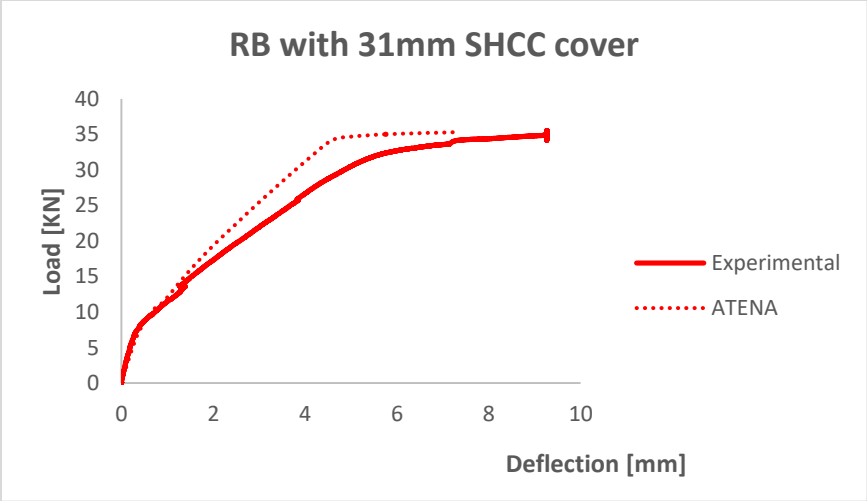

Figure 4.19 Comparison of Load vs Deflection curve for Experimental and Numerical Analysis for RB with 31mm SHCC Cover.

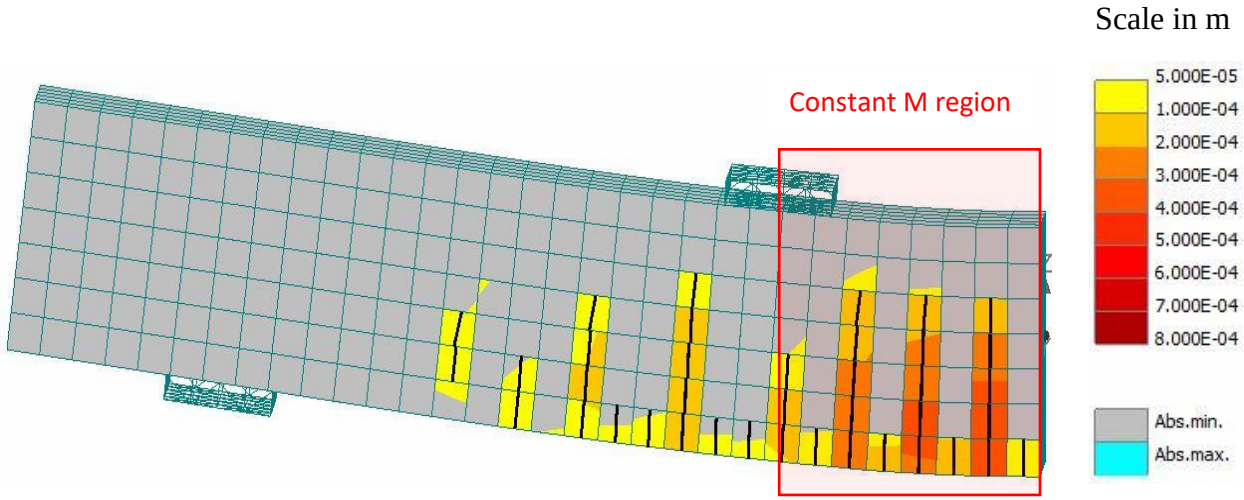

Figure 4.11 Crack pattern of RB with 31mm SHCC Cover at failure load (35.3KN)

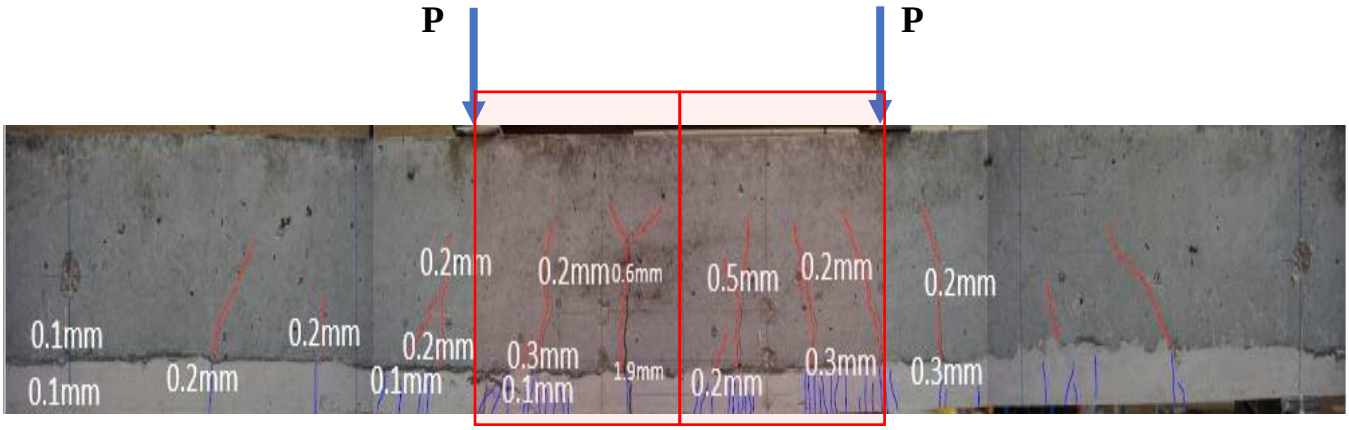

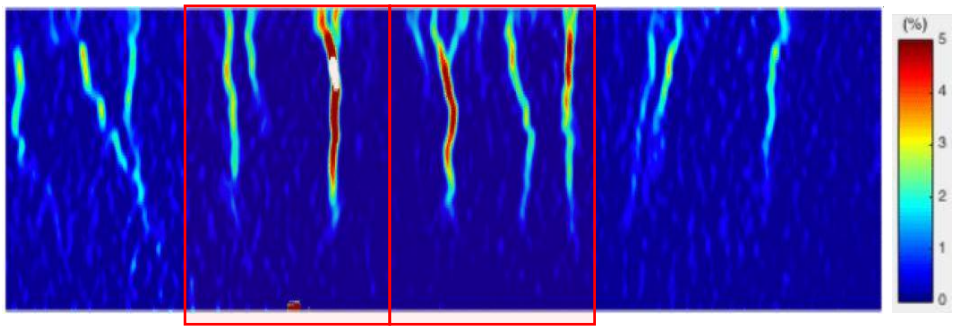

Figure 4.20 Crack Pattern & Strain Energy (εxx) in Cracks obtained from DIC at Failure for RB with 31mm SHCC cover from experimental analysis.

4.3.4 Reinforced Beam with 70mm SHCC Cover.

The same trend is observed also with the increase of the thickness of SHCC layer. Here the difference in stiffness in simulation and experiment is even larger than compared to the smaller thickness SHCC. One of the possible reasons, which will be discussed later, might be the influence of bond between the steel and the concrete, which in the current simulation is simulated as a perfect bond. In really, it might be that this bond is weaker.

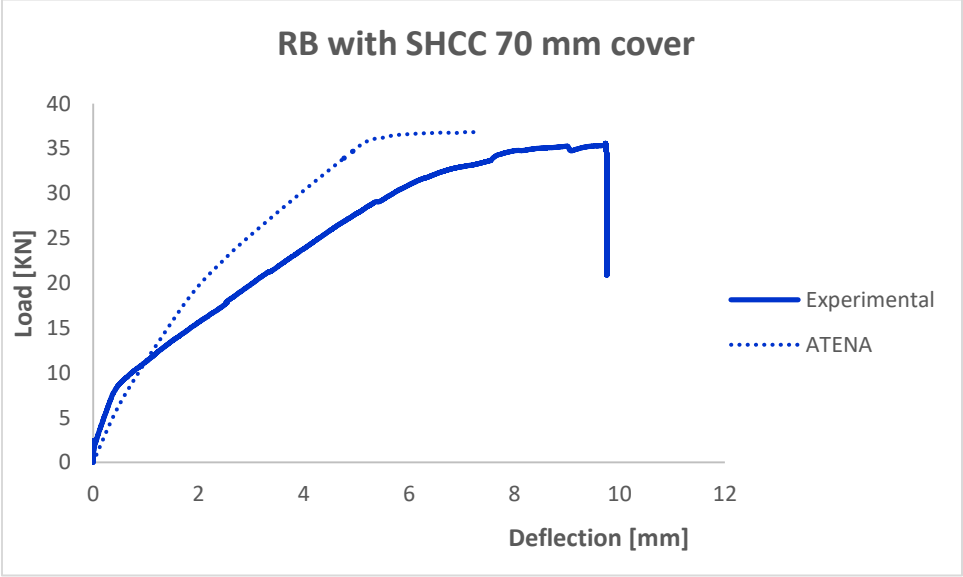

Figure 4.21 Comparison of Load vs Deflection curve for Experimental and Numerical Analysis for RB with 70mm SHCC Cover.

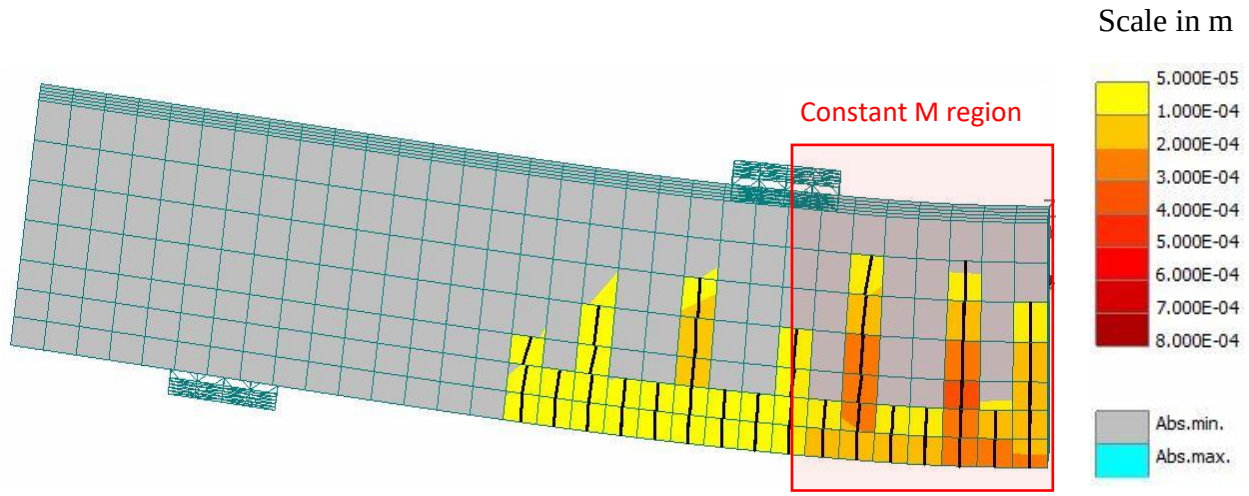

Figure 4.14 Crack pattern of RB with 70mm Reinforcement Cover at failure load (36.8KN)

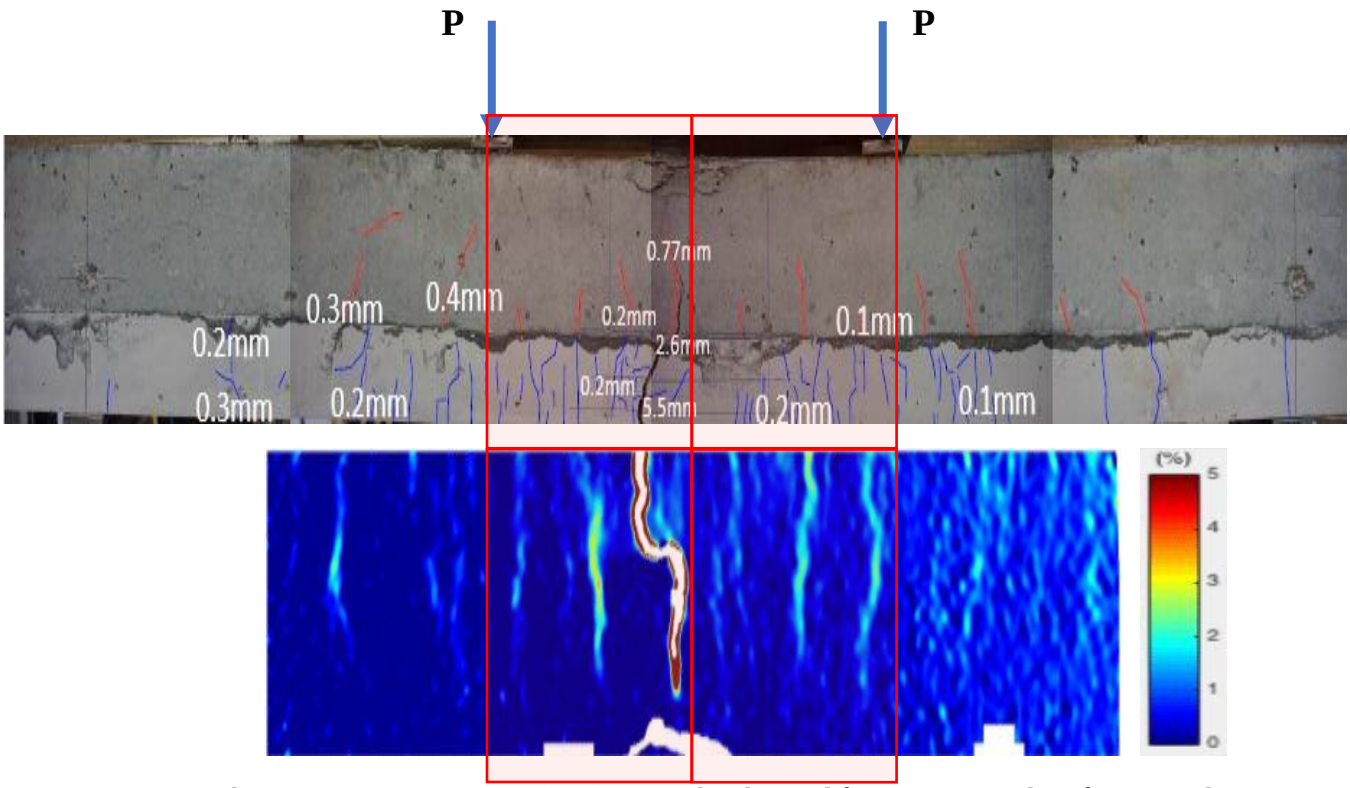

Figure 4.22 Crack Pattern & Strain Energy (εxx) in Cracks obtained from DIC at Failure for RB with 70mm SHCC cover from experimental analysis.

Apart from the above comparisons (where only the deflections are compared), the displacements obtained from the LVDTs from the experiment are also compared with the displacements at the monitoring points defined in the simulations.

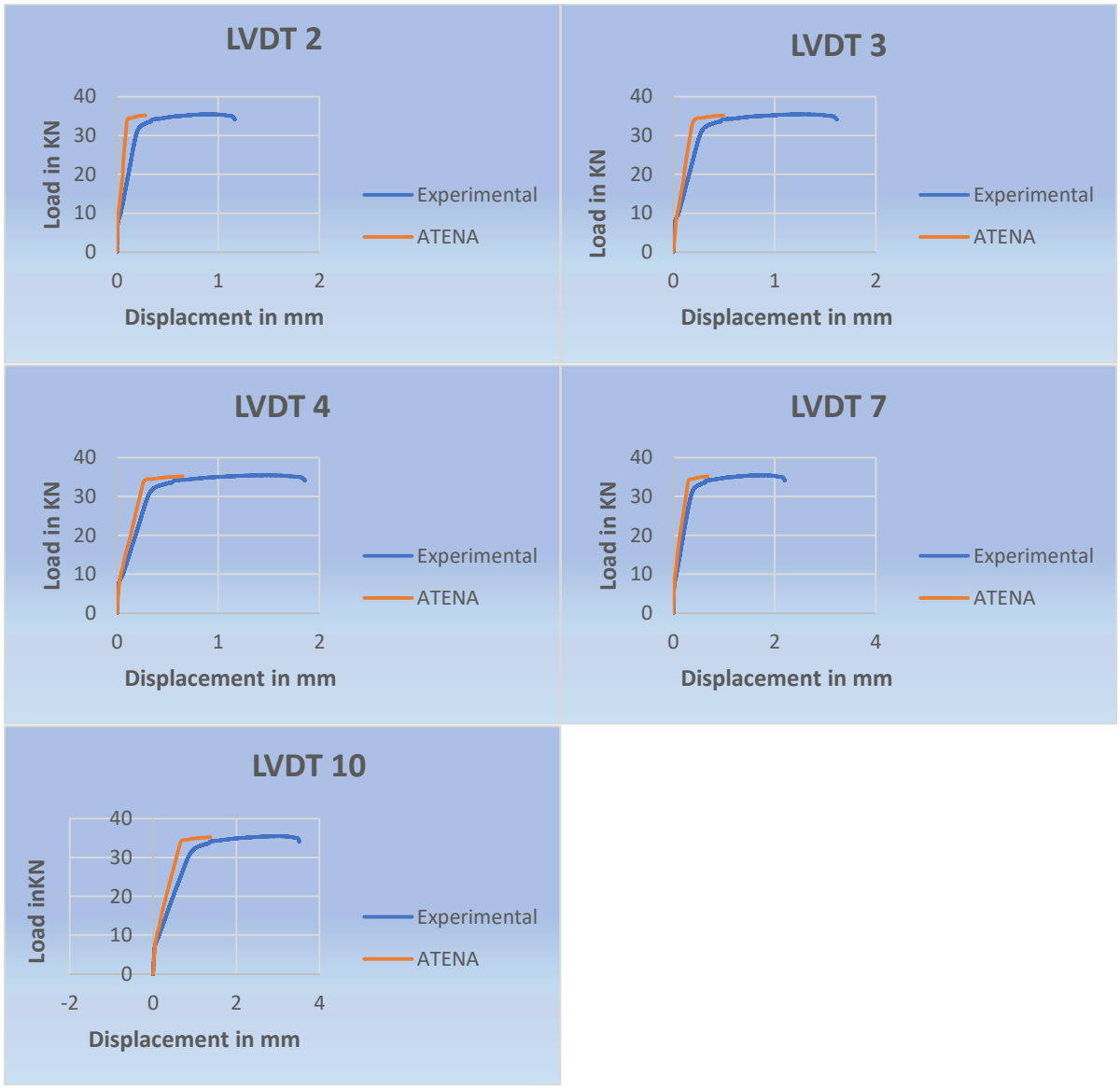

Figure 4.23 Comparison of results from LVDTs and monitoring points from experimental and numerical analysis of RB with 31mm SHCC cover.

4.4 Influence of Bond between SHCC and NSC.

The bond between the NSC and SHCC layers might have a significant influence on the behavior of the beam. The crack pattern – width and spacing is largely affected by the strength of the bond between the above mentioned layers. Therefore a study on the influence of this bond is important. Interface is usually an inherently weak zone, with a high probability of cracking when exposed to a complex stress and strain state caused by incompatibility in properties between the two materials. If the interface is very strong, however, high constraint levels might lead to more cracks in the two materials. Consequently, interface properties at the contact between the two materials will significantly affect the performance of the structure and determine its potential failure pattern [7].

The influence of bond between the two concrete layers has an important role to play in repair systems. In repair systems, ductility and serviceability of the repairing material is of prime importance. As seen from the results in this research, SHCC can be highly beneficial as a repair material. But the bond between the repair material and the defective concrete layer has a significant effect on the efficiency of the repair [7].

A perfect/strong bond between the repair material (SHCC) and the concrete substrate may not be ideally beneficial to the repair system. A perfect bond will ensure that the two layers behave monolithically. Due to this the cracks formed in the concrete layer will propagate directly in to the repair material thereby reducing the efficiency of the repair. On the contrary a comparatively weaker bond but with sufficient strength to prevent failure of the system will provide the required ductility and serviceability to the repair system. A weaker bond will make sure that the repair material is less restrained. Due to the delamination at the interface, there is no sufficient mechanical interlocking between the two layers to suffice the crack propagation and localization. Consequently repair material will form a narrow network of cracks with small crack widths. Thereby increasing the ductility and serviceability [7].

The influence of bond has been tried to understand by using a Lattice model [7]. In this research similar effort is made using the ATENA (Finite element) model to investigate similar behaviors obtained from the Lattice model.

All the previous results have been obtained using the default ‘Perfect bond’ between the two layers. The degree of connection between the layers can be adjusted using the definition of contacts as shown in Figure 4.24.

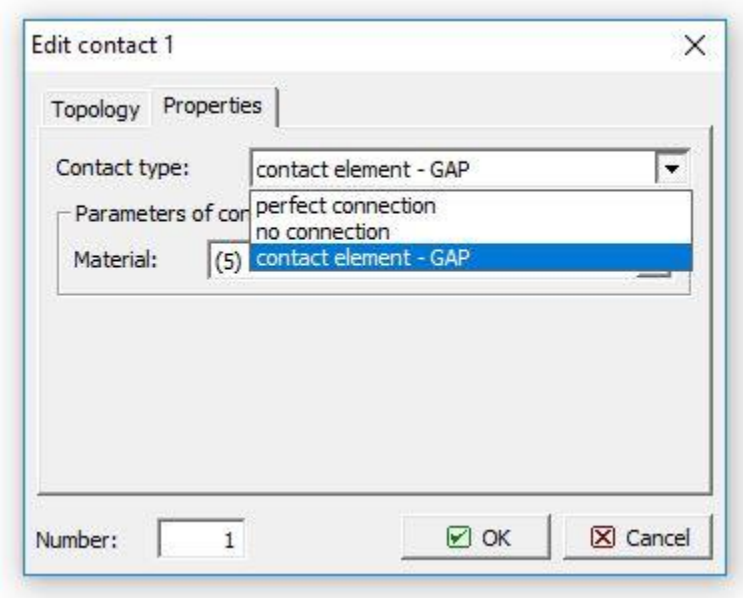

Figure 4.24 Definition of Contact properties

Here, we have three types of connections – 1. Perfect Connection (Full Strength), 2. No connection (Zero Strength) and 3. Contact Element – GAP.

The Contact element can defined using a 3D Interface material. This material can be used to define a connection of the user’s choice.

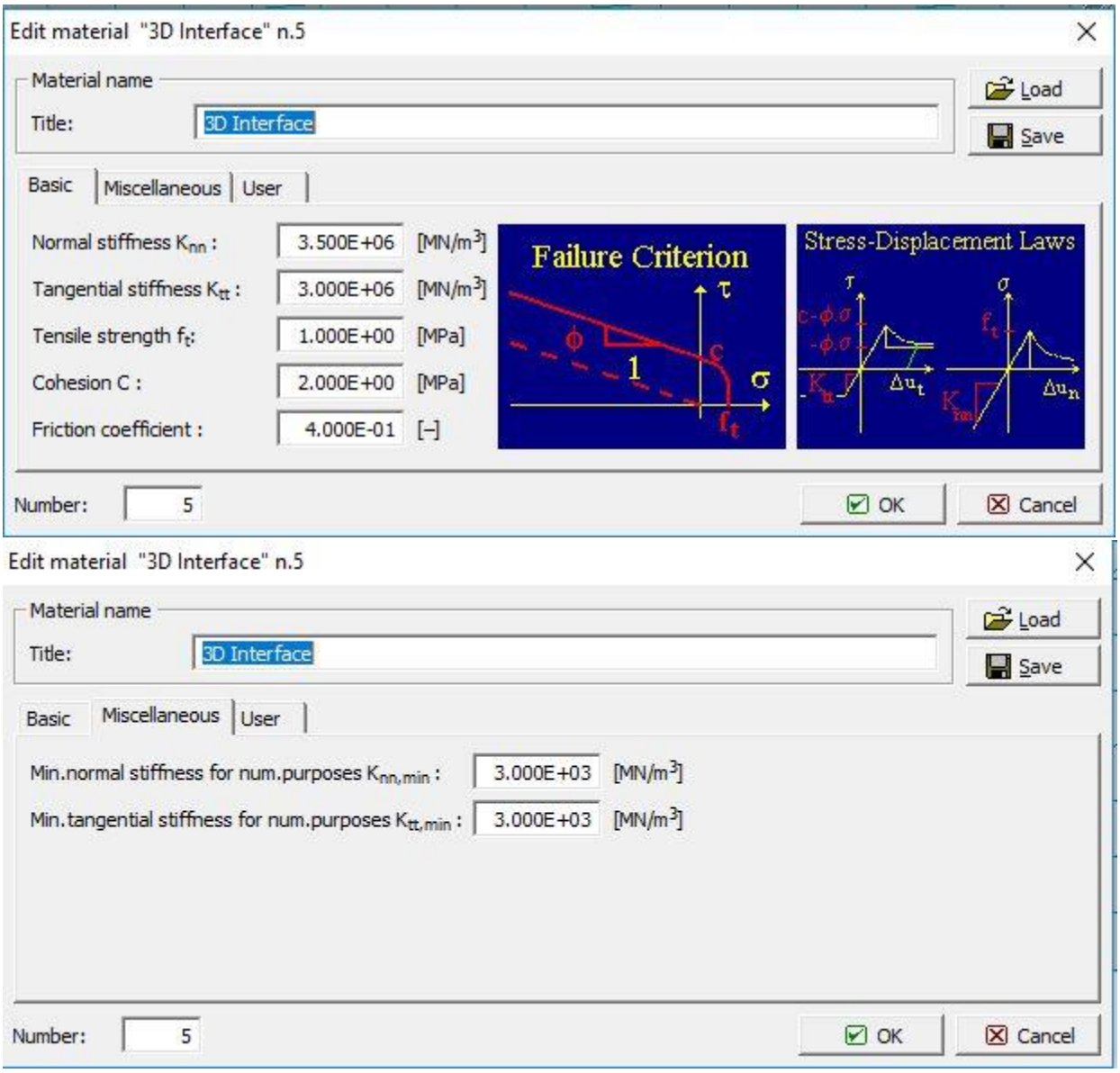

Figure 4.25 Definition of 3D Interface Material for user defined connection between the concrete layers.

The model has two types of parameters. First set of parameters is describing the real physical properties of interface: tensile strength f_t, shear cohesion c, and friction coefficient. They must correspond to real material properties.

The second set of parameters is stiffness coefficients, which serve purely for numerical purposes. There are two stiffness coefficients, K_{nn} (normal), K_{tt} (shear) and each has two values: basic (in closed state, included in menu **Basic**), minimal (in open state, included in menu **Miscellaneous**). The unit of these stiffness coefficients is stress per unit displacement (MPa/m, or MN/m^3).

Theoretically, the basic stiffness should be very high in order to represent well the rigid body and the minimum stiffness should be near zero in order to represent the open contact. However, in practical numerical solutions these values must be reasonably set to allow a stable convergence. In case of difficulties, following rules may be applied: (1) the basic (maximal) stiffness should be about 10 times of the stiffness of adjacent finite elements. (2) Minimal stiffness should be 0.001 times of the maximal stiffness [10] [11].

If the interface tensile strength (f_t) is higher or equal than the f_t of the weaker of the materials being connected with it, it does not make much sense to model such the Interface at all. Then, a perfect connection can be used instead, because the concrete or next to the interface cracks under the same load as the interface.
If there is no information about the interface properties and it is only known/expected that the interface is the weakest and it should fail before the concrete next to it cracks, it is suitable to set the Interface f_t to 1/2 or 1/4 of the tensile strength of the weaker material next to the interface. The Interface cohesion C is recommended to be set to 1-2 times the Interface f_t [10].
A weak bond is modelled using the 3D interface material as shown in Figure 4.25. The interface has a tensile strength of 1MPa, which is lower than the tensile of the NSC (2.2MPa)
The aim is to compare all the three types of connections (Perfect Connection, Weak Connection and No connection) for their load capacities and crack patterns. This comparison is made for RB with 31mm SHCC layer.

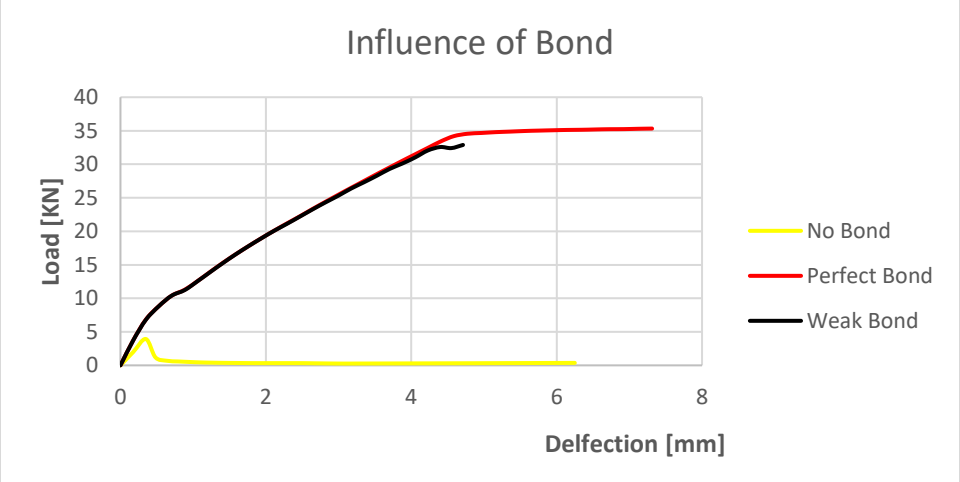

Figure 4.26 Comparison of Load vs Deflections for beams with different type of connections.

From the figure it is clear that the beam with a perfect connection has a higher load capacity than the other two. The beam with no connection has the least load capacity. For the beam with Weak Bond, the analysis stopped half way due to non-

convergence. This can be due to the delamination that occurs at the interface (between the NSC and SHCC) making the structure unstable and outside the region of equilibrium.
However, this does not happen with the beam with no connection. This is probably due to the fact that the 'no connection' setting is a pre-defined model in the programme.

Now comparing the crack pattern at failure for the three types of connections. The crack patterns should be compared at the same step/load to make a valid comparison. Since the beam with weak bond fails at a load of 33 KN. The comparison is made with the perfect bond at the same load step.

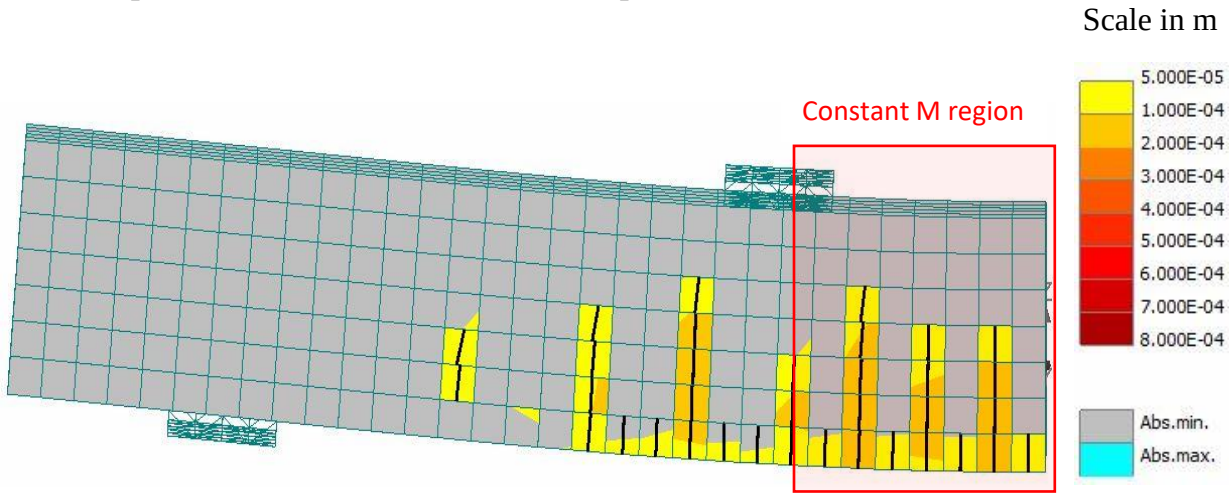

Figure 4.27 Crack Pattern at Load 33KN for RB with 31mm SHCC cover with a Perfect Bond.

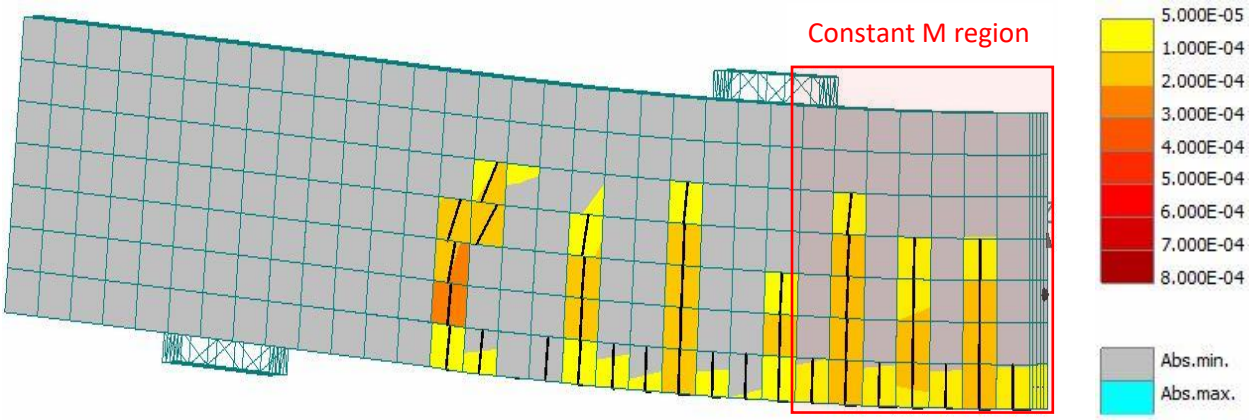

Figure 4.28 Crack Pattern at Load 33KN for RB with 31mm SHCC cover with a Weak Bond

Scale in m

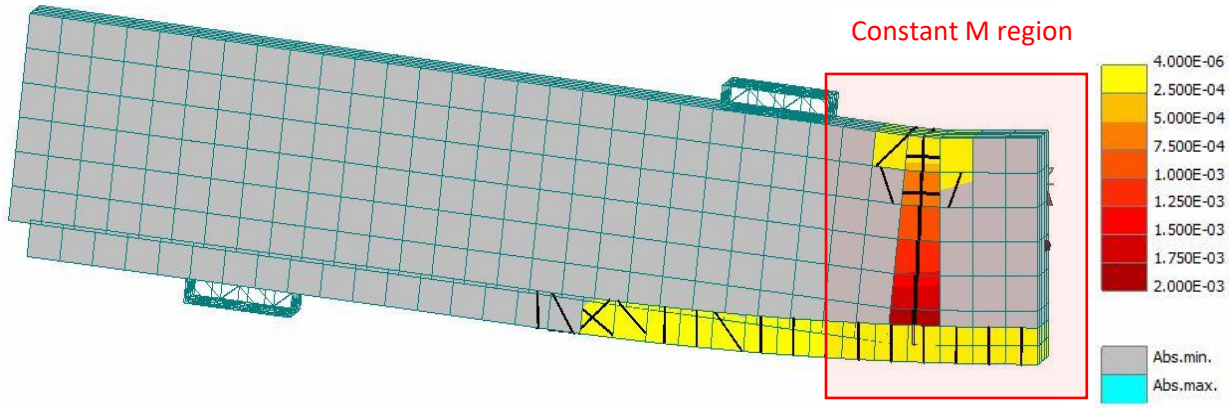

Figure 4.29 Crack Pattern at Failure for RB with 31mm SHCC cover with No Bond.

From the above figures it is clear that for a beam with no bond between the two concrete layers, a delamination at the contact between SHCC and NSC occurs and all the strain is concentrated in a single crack which widens up to 2mm in width and micro-cracking is seen in the SHCC layer with several small cracks developed.

Comparing the perfect and weak bond, a clear distinction cannot be identified although for a beam with weak bond the cracks are slightly more widely spread in the SHCC layer than in the beam with a perfect bond.

However, a delamination at the interface for the beam with a weak bond can be seen by increasing the magnitude of the deformation shown.

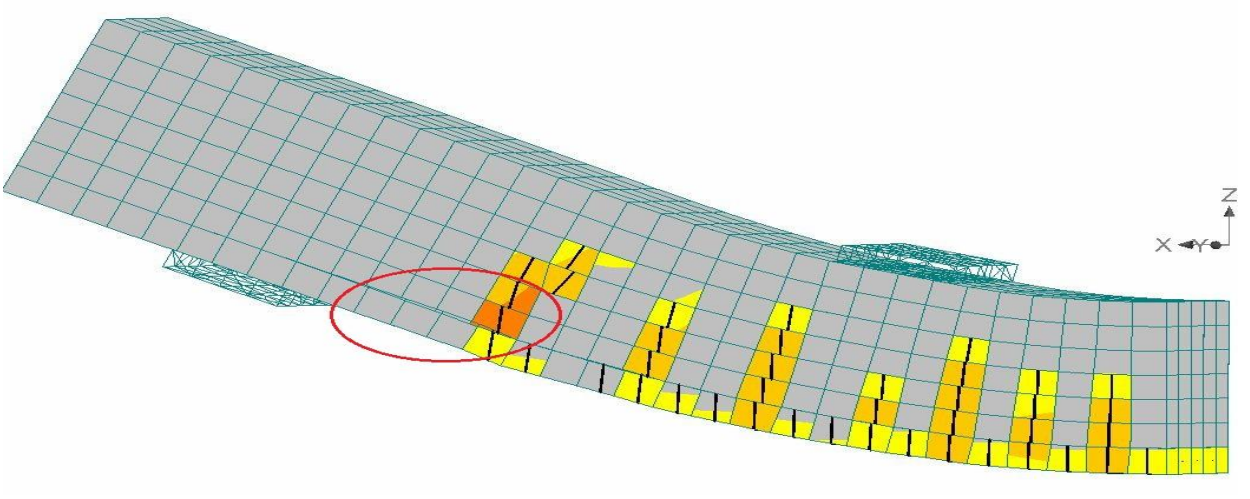

Figure 4.30 Crack pattern of RB with 31mm SHCC cover (weak bond) showing delamination at the interface.

This delamination is absent for the beam with a perfect bond.

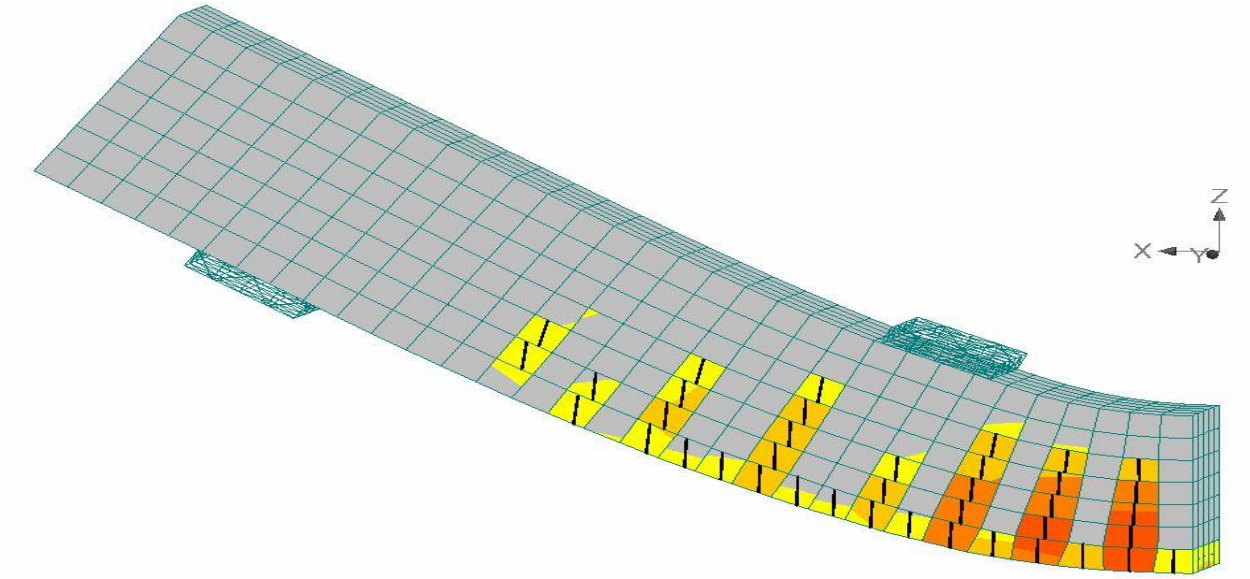

Figure 4.31 Crack pattern of RB with 31mm SHCC cover (perfect bond) without delamination at the interface.

In order to arrive at a clear differentiation and for better understanding of the influence of bond, a mesh refinement study is made. This also enables us to understand the mesh dependency for crack formation.

4.5 Study on Mesh Refinement.

The mesh properties – type and size has an important role in the outcome of a Finite Element analysis. In general, the smaller the mesh size, the closer the FE model is in accord with the real structure. Therefore, a mesh refinement study is important to understand the role of mesh in the FE analysis and its outcome.

In this research, the previous models were constructed using a relatively coarse mesh of 30mm. Now, a single model is chosen say RB with 31mm SHCC cover and the mesh size is reduced to 15mm and the results are compared with the previously used coarse mesh. The programme ATENA is designed to generate one crack per element. Therefore, with a mesh of 15mm, a single crack will be split among two elements to equal the same crack width with a mesh of 30mm.

(The computation time for models with a mesh size of 30mm was approximately 30 mins while the same for a mesh of 15mm was 3-4 hours)

Additionally, another attempt is made to study the influence of the bond properties at the interface using the model with a finer mesh of 15mm size.

First the crack patterns at failure and the deflection profile are compared for a beam with perfect bond for two mesh sizes. Later the influence of bond is studied with the help of mesh refinement.

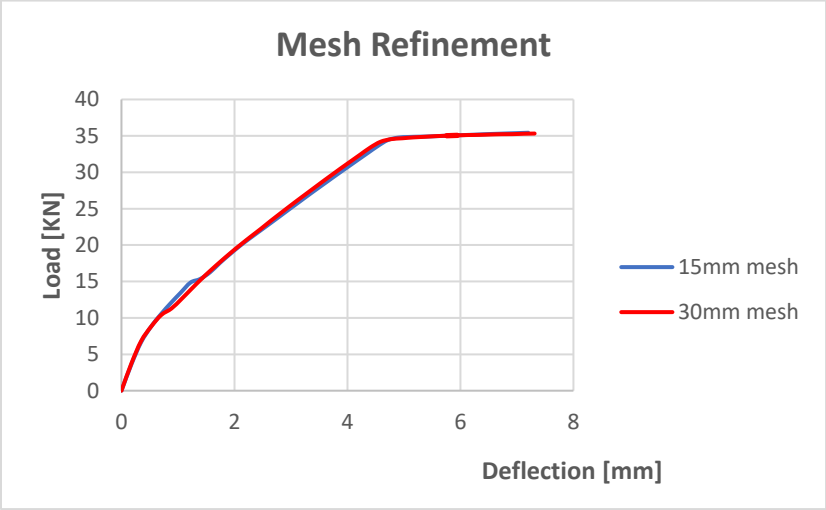

Figure 4.32 Comparison of Load vs Deflection for coarse and fine mesh (RB with 31mm SHCC Cover).

All the Load vs Deflection profile are exactly the same for both the meshes. Still the crack patterns at failure might vary and is checked. Here a minimum crack width of 25 micron is chosen for display.

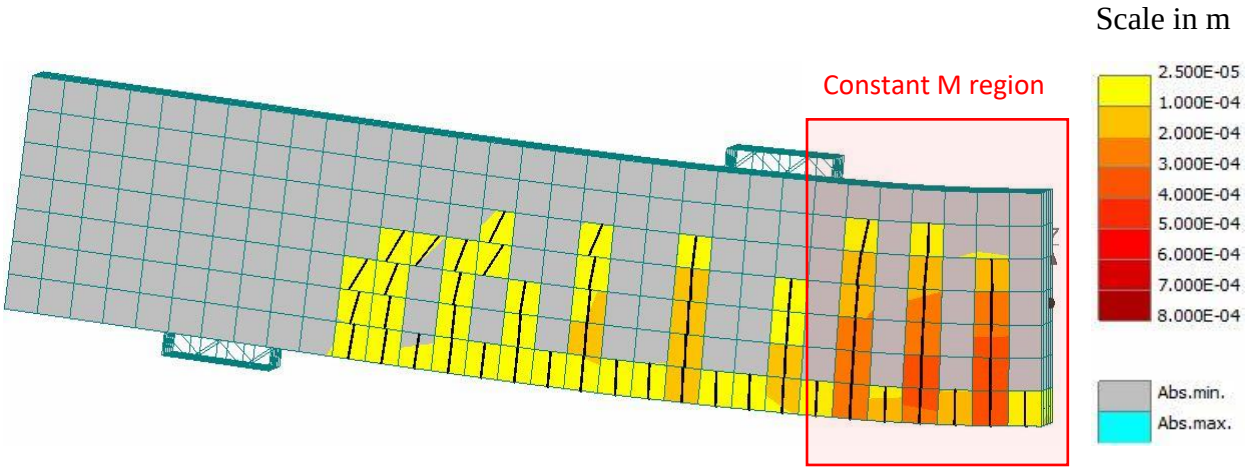

Figure 4.33 Crack pattern at failure for RB with 31mm SHCC cover (30mm mesh).

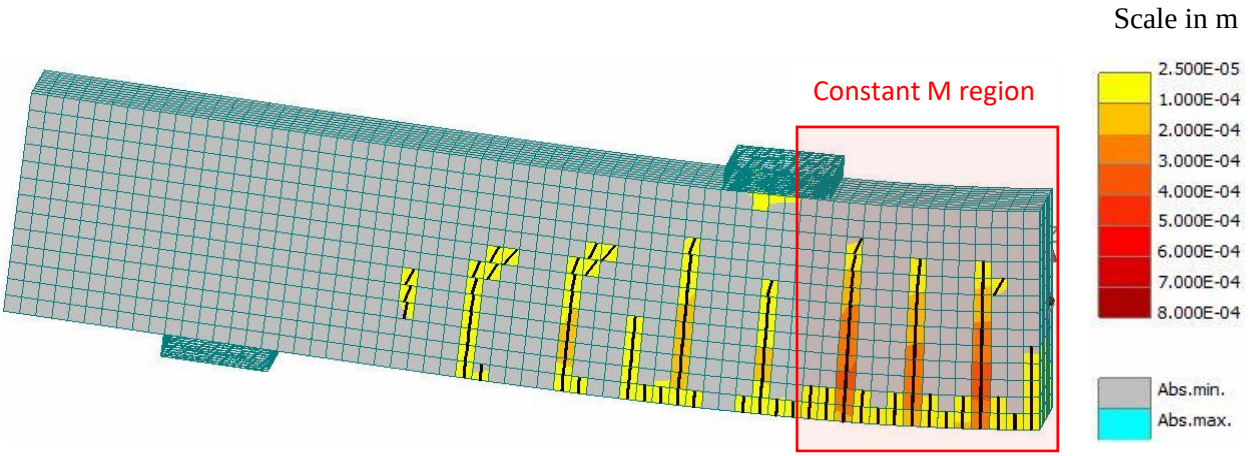

Figure 4.34 Crack pattern at failure for RB with 31mm SHCC cover (15mm mesh).

The above figures gives us a good idea about the influence of mesh properties in the FE analysis. For the beam made using the finer mesh (15mm) a better micro cracking behavior in the SHCC layer can be visualized. The crack pattern for the finer mesh shows many cracks forming a dense network with smaller crack spacing than in the beam with a coarser mesh.

The influence of bond at interface is also studied. Using the finer mesh an attempt is made to obtain a clear distinction between the beam with a perfect bond and the beam with a weak bond. The load capacities and the crack patterns are compared for

both types of bonds. Once again it is important to compare the crack patterns at the same load steps.

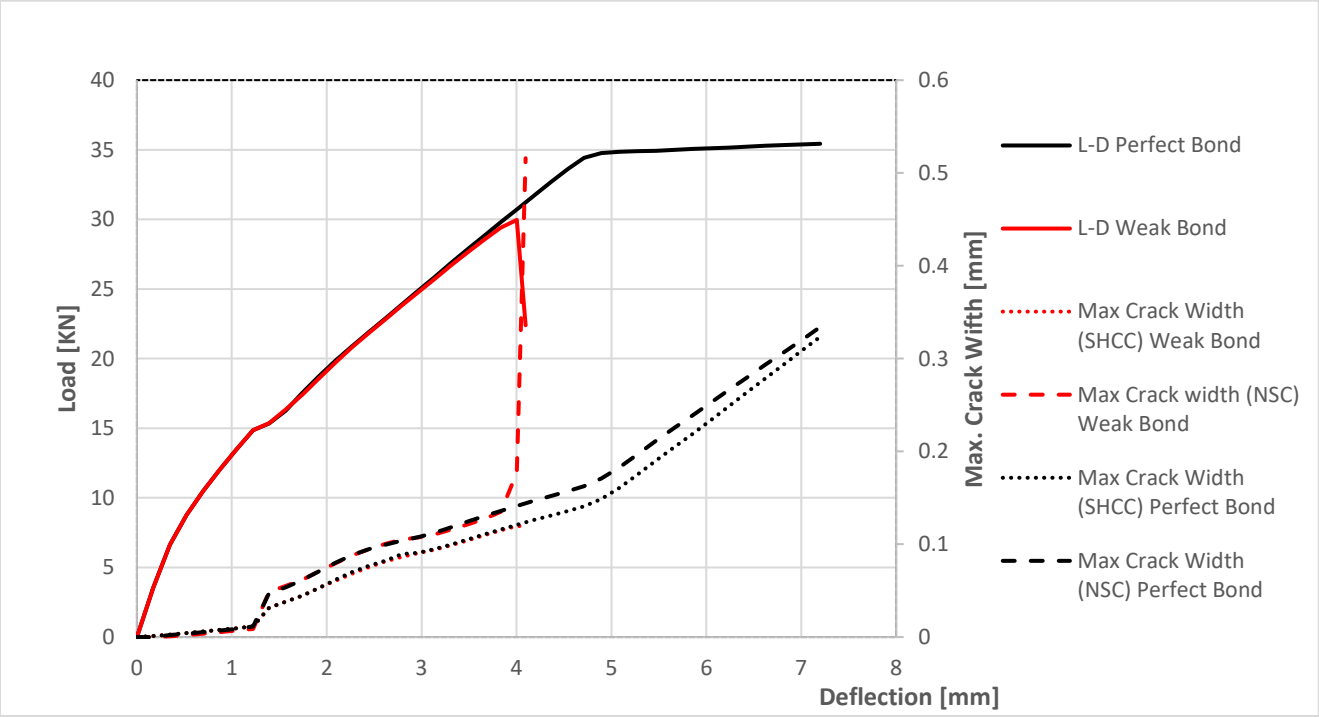

Figure 4.35 Load vs Deflection vs Max. Crack width for perfect and weak bond (15mm mesh).

From the figure it can be seen that the analysis for the beam with weak bond stopped abruptly due to non-convergence. The load vs deflection for both beams follows the same path until the break.

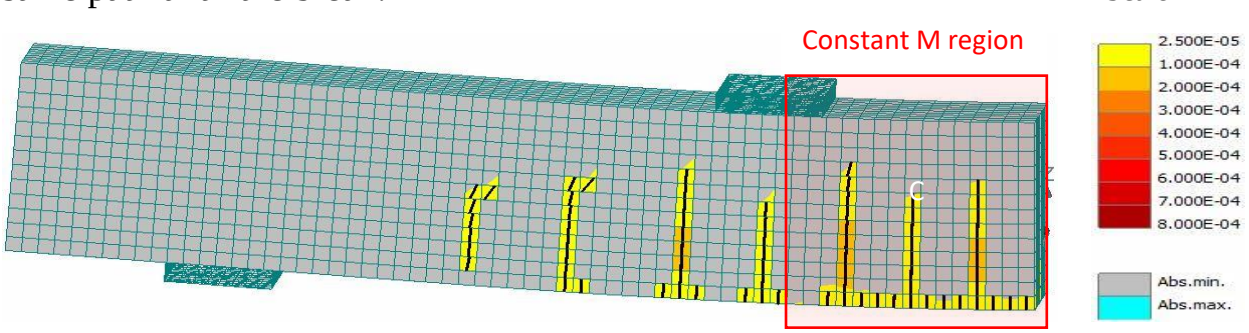

Figure 4.36 Crack pattern at 30KN for RB with 31 SHCC with a perfect bond (15mm mesh).

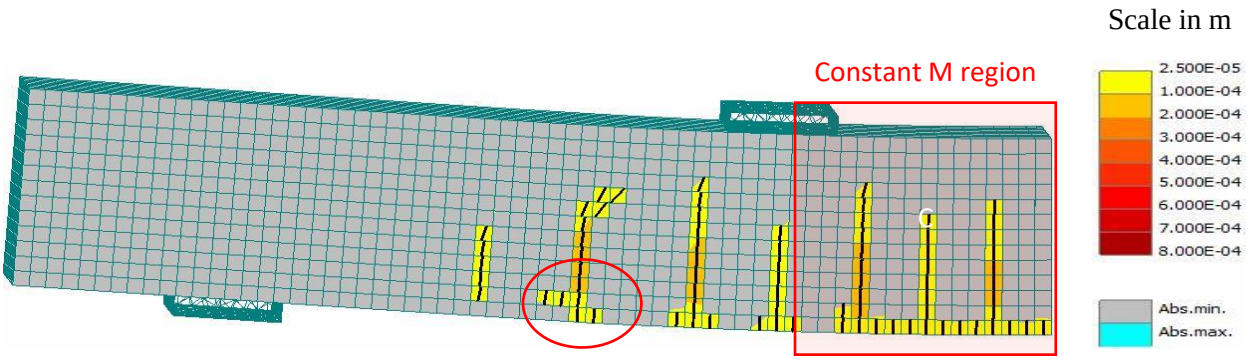

Figure 4.37 Crack pattern at 30KN for RB with 31 SHCC with a weak bond (15mm mesh) and delamination is labelled.

The above two figures show no major differences in crack patterns for beams with different degree of bond at the interface, beside that there is more delamination in the SHCC beam with the weak bond. Comparing the patterns with increased magnitude of deformation as previously done, the delamination at the interface for a beam with weak bond can be obviously seen, which not the case with the beams with perfect bond.

5 Discussions.

The numerical analyses gave mainly satisfactory results. The results from the 4 models of beams gave a clear indication on the benefits of embedding the tensile reinforcement in an SHCC layer.

The comparison of the results from the numerical analyses with that of the experiments performed by Mr. Zhekang Huang showed no major differences between the two types of analyses, concerning the load deformation curves and the flexure capacities of the beams. However, as seen in the comparison of Load vs Deflection graphs (Figure 4.15 & Figure 4.17) the simulation by ATENA shows a stiffer profile when compared with the experimental results. This is also the case for the LVDT graphs (Figure 4.23). Further attention needs to be given to understand this increased stiffness for numerical simulations.

Furthermore, in almost all the beams, the experimental analysis showed crack patterns with lesser number of cracks and higher crack widths than in beams analyzed by numerical simulation. This is clearly evident in the comparison of RB with 70mm SHCC cover, where the maximum crack width is 2.4mm for the beam tested on the experimental set up. Whereas from the numerical simulations the same model shows a maximum crack width of only 0.3mm, which is a big difference. (Figure 4.14 & Figure 4.22)

It is curious to understand why this is the case. One of the reasons could be the influence of bond between the reinforcement and neighboring concrete. The reinforcement has an important significance on the cracking behavior of reinforced concrete beams.

In the numerical analysis the reinforcement bond was taken to be perfect by default. But this may not be the case in reality due to various reasons. Therefore it is important to understand the role of the reinforcement bond - slip behavior on the cracking behavior of the reinforced beam. This may also give us the answer to the above difference between the experimental and numerical results.
Considering this, a beam RB with 31mm reinforcement cover was chosen to study the influence of reinforcement – concrete bond –. The bond properties were changed from perfect to weak using the BIGAJ Bond model. The other option is to use CEB-FIP 1990 model code.
The BIGAJ model is based on the bond strength – slip relationship in the concrete matrix [12].

The modelling of this in the ATENA programme is shown in Figure 5.1.

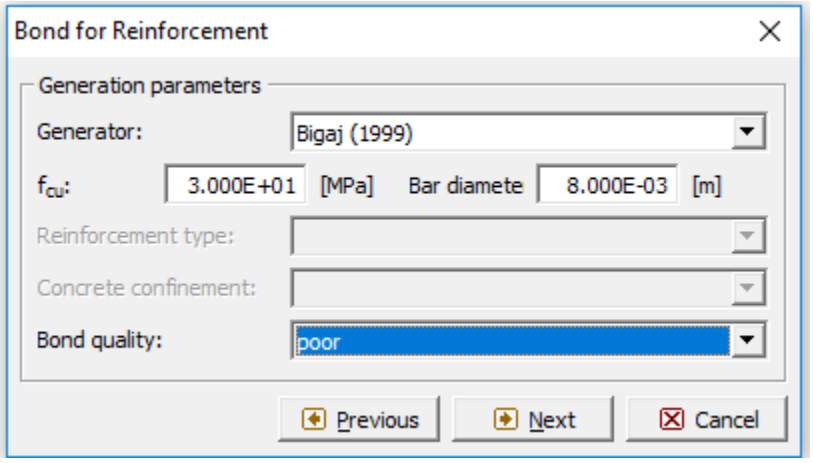

Figure 5.1 Selection of Bond model for Reinforcement.

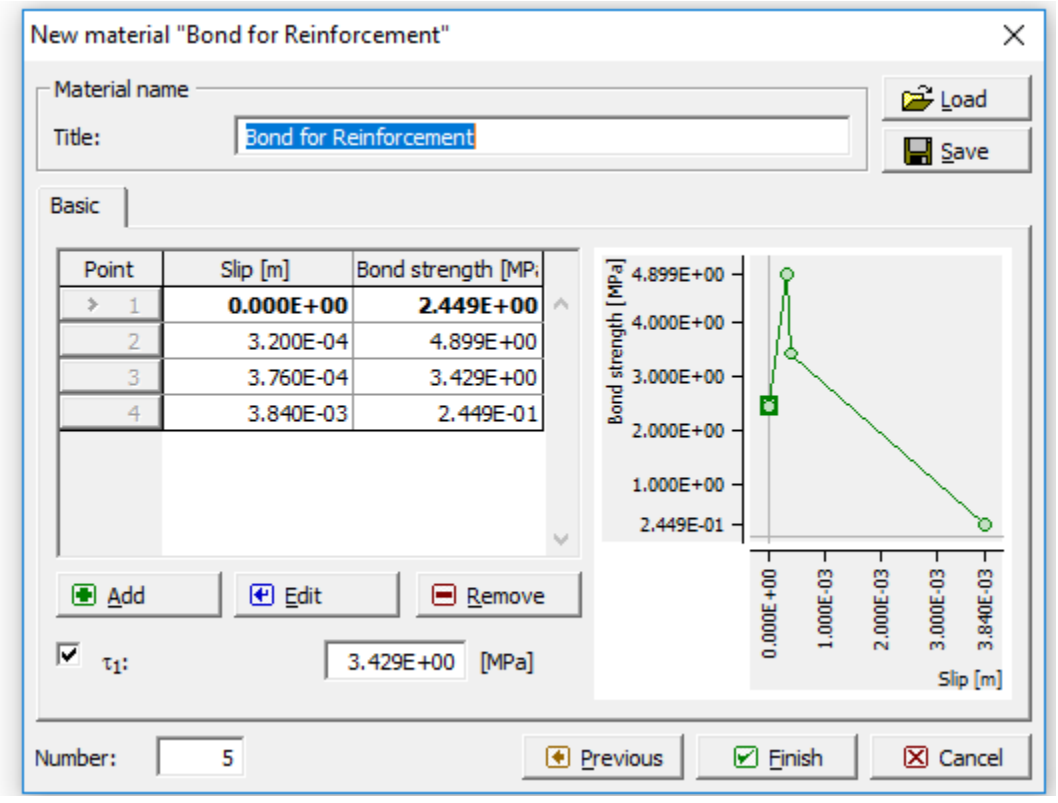

Figure 5.2 Bond strength – slip relationship for a poor bond.

As shown in the figures, a poor bond based on the BIGAJ model was selected and assigned to the reinforcement bars.

The results were compared with the results of beams with a perfect reinforcement bond.

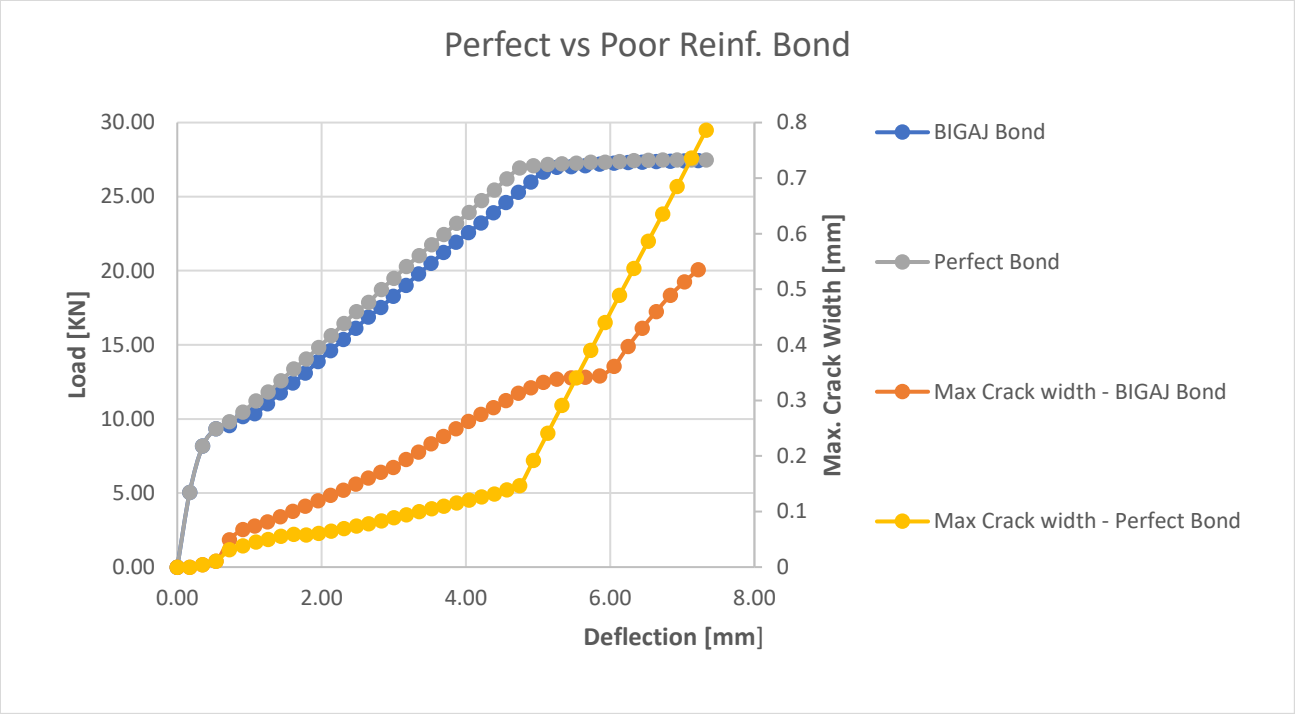

Figure 5.3 Comparison of Load vs Displacement vs Max. Crack width for perfect and poor reiforement bond.

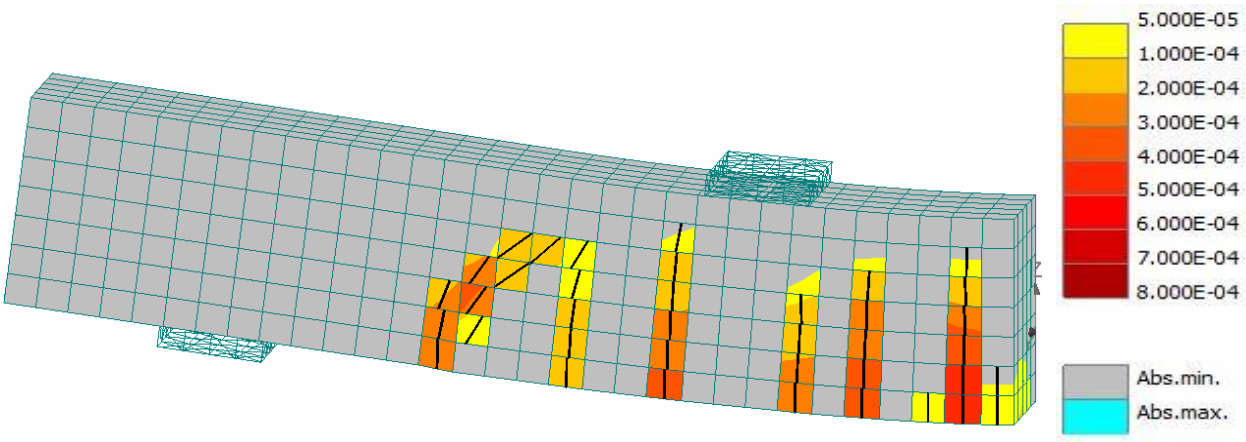

Figure 5.4 Crack Pattern at failure for RB with 31mm cover with BIGAJ Bond for Reinforcement.

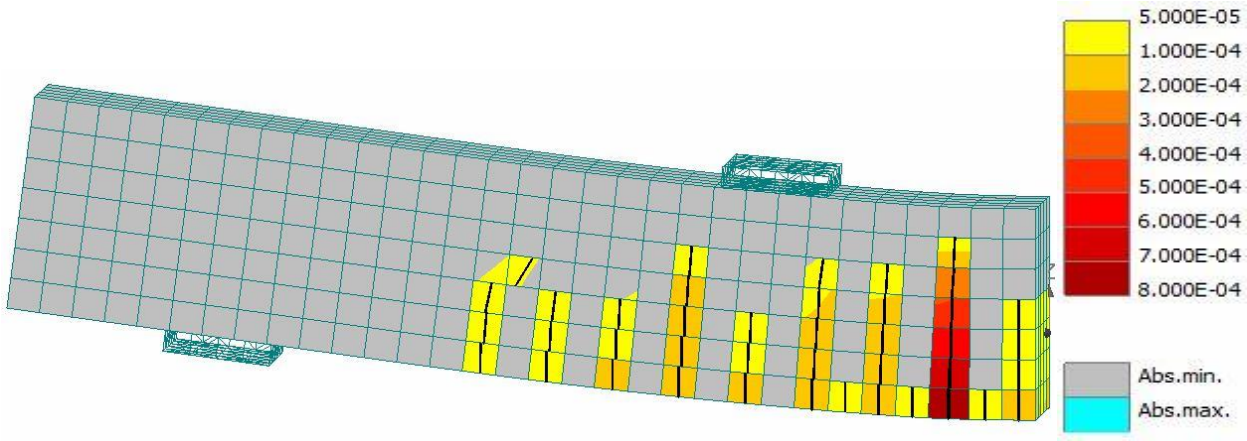

Figure 5.5 Crack pattern of RB with 31mm Reinforcement Cover at failure load for a perfect reinforcement bond.

As we can see, for a perfect reinforcement bond the crack widths in the crack formation stage are significantly smaller than they are in the case of a poor bond (BIGAJ). This is because the bond between the steel reinforcement and surrounding concrete is so good that is does not allow the cracks to open. But at a certain location due to increase in stress concentration, the steel reinforced starts to yield.. No new cracks are formed in this stage and the existing cracks open up as they follow the deformation of steel reinforcement. All the deformation is concentrated at the location of steel yielding and this leads to opening of a single large crack and several small cracks (Figure 5.5).

In comparison, in the beam with a poor reinforcement bond (BIGAJ model in this case) the larger cracks are already formed in the crack formation stage as a consequence of the poor bond which will delaminate allowing the cracks to enlarge (Figure 5.4). Consequently when the steel starts to yield (stabilized cracking), which will happen uniformly due to continuous de-bonding, more or less all the cracks start to open up.

This leaves with a crack pattern of small number of cracks with large crack widths, Which is the case with the beams tested in the experimental set up. The further enlargement of the cracks is because of loading beyond failure.
For both perfect and weak reinforcement-concrete bond, it can be seen that the total deflection is the same.
For a perfect bond, the deflection/deformation will be accommodated by several cracks of small width (but one large crack), whereas in the poor bond, larger cracks

though small in number will be formed. The total crack width (sum of all the cracks in the beam) in both the cased should be theoretically equal since the deflection at failure is the same.

Also, the difference in the stiffness profile in the load – displacement relationship can also be attributed to the influence of bond. As seen in Figure 5.3, the beam with a poor reinforcement bond shows lower stiffness than the beam with a perfect bond.

Similarly, the beam with 70mm SHCC was analyzed with a weak reinforcement-concrete (Now SHCC) bond and the results of both RB with 31mm Cover and RB with 70mm SHCC cover, now with a weak reinforcement bond are compared.

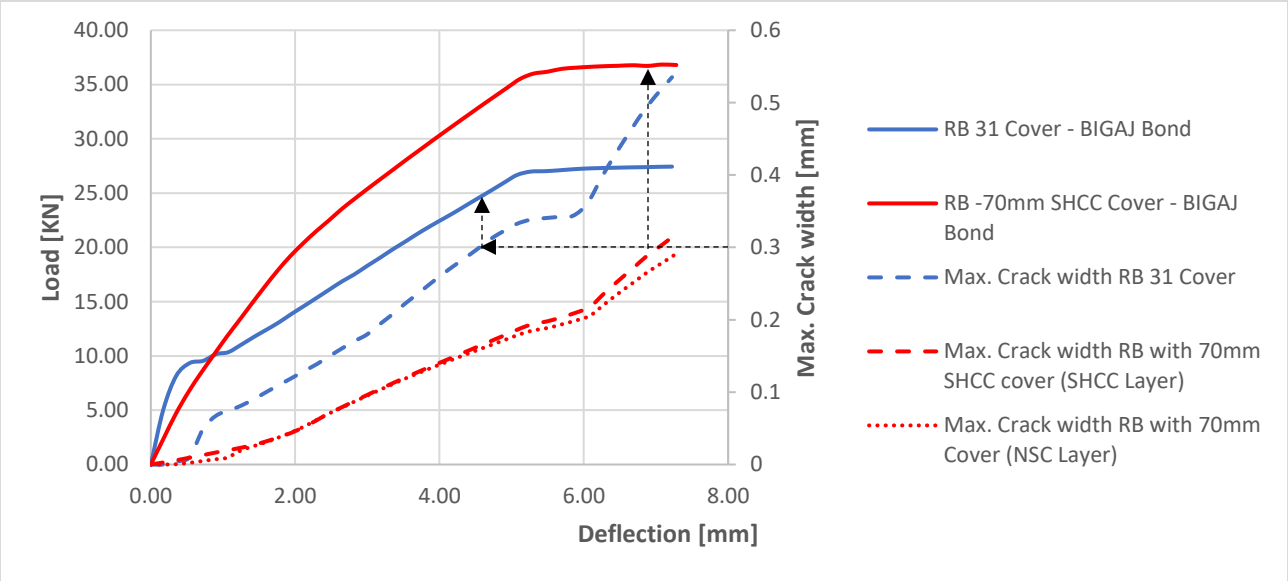

Figure 5.6 Comparison of Load vs Deflection vs Max. Crack width for RB with 31mm cover and RB with 70mm SHCC cover with BIGAJ Bond for reinforcement.

The SHCC beam does not show any difference in behavior with a weak reinforcement bond. The maximum crack width is still the same as it was for a perfect reinforcement bond. From this it can be said that for beams with SHCC the reinforcement bond is not as dominant as the SHCC layer itself in controlling the crack width. Due to its own crack bridging ability the SHCC layer still performs in limiting the crack width irrespective of the reinforcement bond strength. This is not the case with beam with NSC. As clearly seen from Figure 5.6, a crack width of 0.3mm has already opened up in the NSC beam in its stabilized cracking stage.

Whereas for the SHCC beam the same crack width opens up at the failure of the SHCC layer. This is the major difference in behavior of NSC and SHCC.

Finally, these results (with BIGAJ bond) are compared to the experimental results to check if we can find a better closeness between the two results.

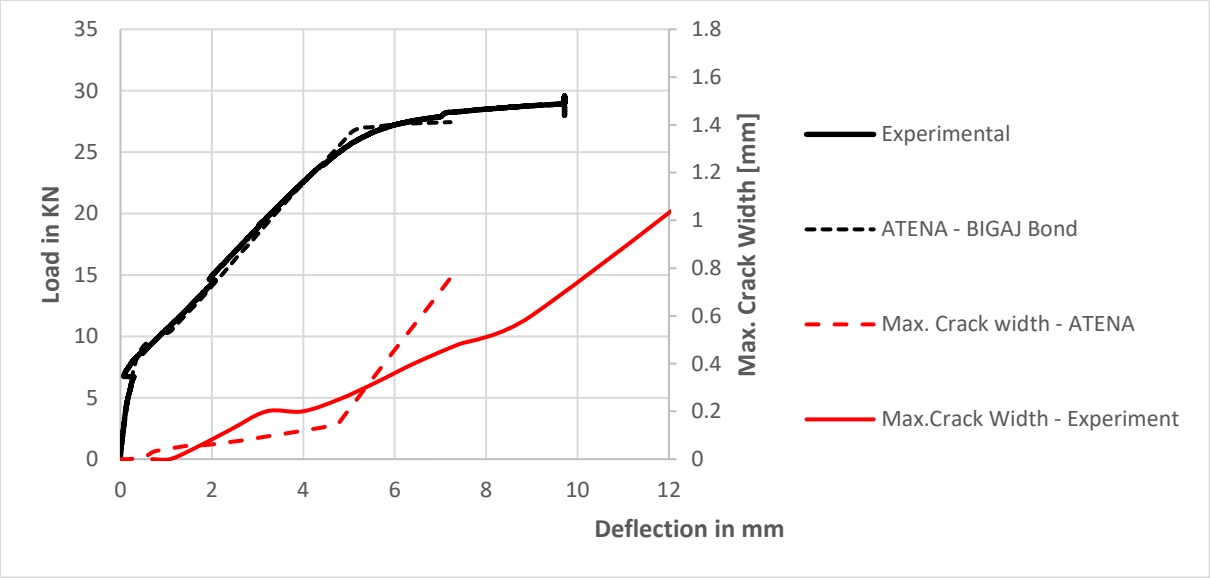

Figure 5.7 Load vs Deflection vs Max. Crack width for RB with 31 mm for Experimental and Numerical (With BIGAJ bond) analysis.

From the above comparison we can see that the load – deflection relationship are almost identical between the two analyses. The crack development shows a reasonable similarity between the two results.

With this we can come to an understanding of how important of an influence the reinforcement –concrete bond has on the behavior of Reinforced Concrete beams.

Furthermore, an attempt made to understand the role of bond between the concrete and SHCC provided some insights into the behavior of the composite beam.

For the beam with no bond at the interface, the difference was obvious which showed a complete delamination at the interface and localization of a single larger crack in the NSC layer and micro cracking in the SHCC layer (Figure 4.29). The peak load (Figure 4.26) for this beam is significantly smaller than for the beams with perfect and weak bond. This due to no mechanical interlocking between the two concrete surfaces, which prevents the propagation of a crack first formed in the NSC layer into the SHCC layer.

The comparison for beams with perfect and weak bond showed a small delamination for the beam with weak bond (Figure 4.30). But the crack patterns remained fairly similar for both types of connections.

In reality, for a perfect bond at the interface the two concrete layers (NSC and SHCC) behave as one material and the crack formed in the NSC layer propagates into the bottom SHCC layer and there it subsequently forms a distributed crack pattern. On the contrary, for the beam with a weak bond at interface, the interface strength is too low to create a strong interlocking between the two materials and the beam behaves more or less as a combination of both no bond and perfect bond. Firstly, the crack that forms in the NSC does not immediately propagate into the SHCC. And since the SHCC layer is not restrained as in the case of a perfect bond, more cracks develop in the SHCC layer with smaller crack widths. But since there is substantial strength in the interface, the peak load is not as low as it is for the beam with no bond at all.

6 Conclusions and Recommendations.

In this research, the benefits of embedding the tensile reinforcement in a layer of SHCC were investigated. This was done by comparing conventionally reinforced beams of a particular reinforcement cover with those of beams with similar covers of SHCC layers.

The results were compared with experimental analysis performed by Mr. Zhekang Huang. Additionally the influence of the bond between the NSC and SHCC layers on the behavior of the beams was studied.

In order to understand the mesh dependency of the FE analysis and mesh refinement was done and the results were compared with the previously obtained results from a coarser mesh size.

The following conclusions and recommendations can be made based on the results obtained in the research.

- The layer of SHCC in the tension zone provides substantiate benefits to the beams in both ULS and SLS stage. For ULS it increases the load carrying capacity. For SLS the smaller cracks and absence of localization of cracks (micro-cracking) is a major advantage over conventionally reinforced beams. The PVA fibers in the SHCC layer are responsible for this behavior, who with their crack bridging ability shift the stress concentration responsible for opening of cracks resulting in formation of new cracks at another location. Thus, preventing localization of cracks and possibly improving durability of the concrete structures..
- The beam with a reinforcement cover of 31mm has the least load capacity. This is due to the reduced bending capacity due to decreased internal lever arm as compared to the beam 11mm reinforcement cover. The simulated maximum crack width at the failure in this beam is around 0.8mm, which is around 2-3 times smaller than the experimentally obtained value.
- Out of the four beams considered, the beam which performs the best both under ULS and SLS stage is the beam with reinforcement embedded in 70mm cover of SHCC. The maximum crack width in this beam is limited to 0.3mm and has a peak load of 37KN (Half of Peak Load for a full length beam).
- The comparison of results from numerical simulations using ATENA and experimental observations showed no major differences in the load capacities of the beams. However, the profile of Load vs Deflections shows us an

increased stiffness for numerical results. As seen from the previous chapter the reason for this could be the influence of reinforcement bond.

- The crack patterns obtained from both numerical analysis and experimental analysis show differences in both number and widths of cracks. In the experiment lesser number of larger cracks can be seen. On the contrary, for the numerical simulation higher number of smaller cracks are formed. Once again the reinforcement bond plays a major role in this indifference as seen from the previous chapter.
- Study on influence of bond between the NSC and SHCC did not show large influence on crack widths. Nevertheless, it leaves with an opportunity in the future to precisely model an interface with the other type of model and see if the effect would be the same.
- The study on mesh refinement enabled to understand the mesh dependency of the finite element analysis. By comparing the crack patterns from a coarser mesh and a finer mesh, it can be seen that because of mesh dependency of the crack formation (one crack per element) the micro – cracking behavior of the SHCC is not precisely shown. This behavior can be clearly seen in the crack patterns obtained using a finer mesh.

In this research, the SHCC was modelled solely based on its tensile hardening function. But another important aspect of SHCC which contributes to the tensile hardening of SHCC, is the fibers (PVA) and their orientation in the cement mixture. The fibers' crack bridging ability is largely enhanced when they are oriented horizontally. Although this alignment may be achieved with smaller thicknesses of covers, it becomes difficult to ensure the alignment when the cover has a larger thickness (e.g. a cover of 70mm SHCC as used in this research). Therefore further knowledge on how the SHCC can be modelled by incorporating these aspects of the fibers is necessary for future reference.

7 References

[1] V. Li, S. Wang and C. Wu, *Tensile-Strain hardening behavior of polyvinyl alcohol engineered cementitious composites (PVA - ECC),* ACI Materials Journal, 98(2001).

[2] V. Mechtcherine and J. Schulze, *Ultra-Ductile Concrete - Material Design Concept and Testing,* CPI Concrete Plant - International, 2005.

[3] F. d. A. Silvaa, M. Butler, V. Mechtcherine, D. Zhub and M. Barzin, *MECHANICAL BEHAVIOUR OF STRAIN-HARDENING CEMENT-BASED COMPOSITES (SHCC) UNDER LOW AND HIGH TENSILE STRAIN RATES.*

[4] T. Rokugo, T. Kanda, T. Kanakubo, P. Kabele, H. Fukuyama, Y. Uchida, H. Suwada and v. Slowik, "Strain Hardening Cement Composites - Structural Design and Performance".

[5] "Yuva Engineers," [Online]. Available: http://www.yuvaengineers.com/engineered-cementitious-composite-ecc-the-bendableconcrete/.

[6] V. C. Li, *Engineered Cementitious Composite (ECC) - Material, Structural, and Durability,* University of Michigan, August 2007.

[7] M. Luković, "INLUENCE OF INTERFACE AND STRAIN HARDENING CEMENTITIOUS COMPOSITE PROPERTIES ON PERFORMANCE OF CONCRETE".

[8] G. Fischer, *Mechanical characterization and testing of Strain-Hardening Fiber-Reinforced Cement Based Composites (SHCC),* Technical University of Denmark, Decemeber 2011.

[9] F. Leenders, "Integral Abutment Bridge and Strain Hardening Composites," Delft University of Technology, November 2014.

[10] "ATENA Troubleshooting," [Online]. Available: http://www.cervenka.cz/assets/files/atena-pdf/ATENATroubleshooting..

[11] V. Cervenka, L. Jendele and J. Cervenka, *ATENA Program Documentation, Part 1, Theory,* Cervenaka Consulting, 2016.

[12] L. Jendele and J. Cervenka, *Finite Element Modelling of Reinforcment with bond.*

[13] [Online]. Available: http://www.yuvaengineers.com/engineered-cementitious-composite-ecc-the-bendableconcrete/.

[14] "Cervenka Consulting Web," 2013. [Online]. Available: www.cervenka.cz/.

[15] J. Cervenka and Z. Procházková, *ATENA Program Documentation, Part 4-2 Tutorial for ATENA 3D*, Cervenka Consulting, 2016.

[16] V. Cervenka and J. Cervenka, *ATENA Program Documentation, Part 2-2, Manual for ATENA 3D*, Cervenka Consulting, 2017.

[17] V. Cervenka and J. Cervenka, *ATENA Program Documentation, Part 2-1, Manual for ATENA - 2D*, Cervenka Consulting, 2011.